MARTIN NUCLEAR

DISCLAIMER

SNAP 19

TEST REPORT

THERMAL PERFORMANCE OF MATERIALS

AND MECHANICAL JOINTS

MND-3607-112

November 1966

Prepared by: _____
C. Shih

Approved by: _____
J. Jicha

_____
J. L. Powell, Jr.

LEGAL NOTICE

FOREWORD

This test report is submitted by the Martin Company, Baltimore, Maryland, a division of the Martin Marietta Corporation, in support of United States Atomic Energy Commission Contract AT(30-1)-3607, Item (4) (1) (h), of the SNAP 19 Experimental Program.

ACKNOWLEDGMENT

Blank

CONTENTS

Blank

SUMMARY

The purpose of this program was to provide basic information on the thermal contact conductance of mechanical joints for application to Nimbus B/SNAP 19 thermal analysis and to gain knowledge of the proper joint thermal conductance in scaled thermal models. A secondary objective was to evaluate material properties such as the coefficient of thermal expansion, thermal conductivity, emissivity, specific heat, and tensile and creep strengths at temperatures from 300° to 783° K. No such information at temperatures above 400° K is available in the literature.

For the joint conductance study, three specimens of ZH62A Mg alloy against 2024-T5Al alloy, the same materials as those used on Nimbus B spacecraft, were fabricated. One used a hexagonal-head bolt, one a countersunk head bolt and one a rivet as fasteners. All three specimens were of approximately the same size as the proto-type. Thermal conductances were evaluated at four different temperatures ranging from 340° to 566° K for each load and environment pressure.

For thermal scaling of joint thermal conductance, two more specimens of stainless steel were fabricated, one approximately the same size as those used on the Nimbus B spacecraft and the other a half-scale model. The steel specimens were tested under environmental conditions identical to those experienced by the Mg-Al specimens.

Contact thermal conductances of joints, typical of those used on the Nimbus B spacecraft, were measured at various temperatures, both with and without a special grease between the surfaces of contact. The measured thermal conductances of all joints with grease coated surfaces are higher by almost an order of magnitude than the minimum value given by General Electric specifications. One of the specimens tested showed some characteristics not common to all the rest, possibly due to inaccuracy as a result of the small temperature drop across the joint under greased conditions. Thermal scaling of mechanical joints was proven to be quite feasible within the scope of interest to the Thermal Scale Model Program (Task 4.1.a). Using the thermal scaling criteria given in Ref. 1, scaling of material properties was within 11% at all temperatures tested. With respect to scaling to size, the experimental results agree with the criterion within 18%. The agreement of experimental results with criterion for scaling of a greased joint is about 23%. For thermal conductance of mechanical joints with a grease interface, a tolerance of 50% is recommended for thermal design purposes, due to uncertainties about the effects of temperature, pressure and time of exposure in vacuum on the thickness and density of the grease.

Material properties at various temperatures were determined follow-
ing ASTM standard procedures. There was some uncertainty about the
thermal conductivity and creep strength at temperatures close to the
melting point. Verification tests of thermal conductivity of ZH62A were
simultaneously carried out at both the Nuclear Research Laboratory
and the Thermodynamics Laboratory. Some scattering of test results
was noted around 770° K. Values in the temperature region from 740° K
up should be used with caution.

Recommendations were made to investigate anomalies in the creep
strength data and to supplement the data obtained on thermal conduct-
ance of mechanical joints.

Tests of typical properties at elevated temperatures are summa-
rized

Property	Temperature (° K)				
	300	554	610	672	700
Thermal Conductivity $(cal/cm^2-sec-(°K/cm))$		0.33	0.285	0.265	0.258
Specific Heat $(cal/gm-°K)$			0.261	0.318	0.335
Coefficient of Expansion $(micro-cm/cm-°K)$	23	29	29.5	29.5	29.5
Total Hemispherical Emittance		0.111		0.116	
Total Normal Emittance			0.80		0.90
Tensile Strength (Kg/cm^2)					
Ultimate	2510	935	680	422	317
Yield	1554	618	571	317	260

SYMBOLS AND DEFINITIONS

a	radius of microscopic contact area (meter)
A	surface area (meter^2)
b	radius of macroscopic contact area (meter)
d	thickness (meter)
E	modulus of elasticity (Newton/meter^2)
h_{ij}	thermal contact conductance (joule/meter^2-sec-°K)
H	microhardness of material (Newton/meter^2)
K	thermal conductivity (joule/(meter^2-sec-°K/meter))
L	linear dimensions (meter)
P_a	pressure over apparent contact surface area (Newton/meter^2)
R	contact thermal resistance (sec-°K/joule)
s	peak to valley surface deviation (meter)
T	temperature (°K)
q	rate of heat transfer (joule/sec)

Subscripts

i, j	quantities associated with surfaces in contact with A_i and A_j, respectively
m, p	quantities associated with the model and the prototype, respectively
t	total value
mi, ma	quantities associated with microscopic and macroscopic phenomena, respectively

I. INTRODUCTION

The thermal performance of a spacecraft in re-entry depends a great deal on the thermal conductance through various mechanical joints. In some instances a joint must be designed for maximum thermal resistance to prevent heat leakage such as in cryogenic storage. In other applications, the joint has to be designed for minimum thermal resistance so that the heat dissipation from certain areas can be facilitated. To our best knowledge, the work done on contact thermal conductance has been limited to the measurement of conductance between plane surfaces under given temperature conditions and surface finishes. No work on scaling of thermal conductance has been reported. In order to have a good representative thermal model of the Nimbus B vehicle, it is essential that a good knowledge of the thermal conductance of mechanical joints used in the spacecraft be obtained.

There is also a lack of knowledge of the general thermal and mechanical properties of magnesium or magnesium thorium alloy at temperatures near the melting point.

The objective of this program is to evaluate the thermal contact conductance of mechanical joints typical of those in the Nimbus B satellite sensory ring and to determine some of the physical and thermal properties of magnesium alloy ZH62A at higher temperatures. These are not available in the literature. To effectively attain these goals, the program was divided into two subtasks: the joint thermal contact conductance study carried out by the Thermodynamics Laboratory and the material properties study carried out by the Materials Engineering Laboratories.

Five specimens were fabricated and tested in the joint thermal contact conductance study. Three of the specimens, one each with a hexagonal-head bolt fastener, countersunk machine screw fastener and riveted fastener, were made with ZH62A and Al 2024-T4 forming the mating surfaces. A construction typical of that used in the Nimbus B sensory ring assembly was employed. A fourth specimen was made with Type 304 stainless steel forming the mating surfaces for thermal scaling when changing materials. A fifth specimen which was a reduced scale of the fourth specimen was used for thermal scaling in size. The contact conductances of the joints were measured at temperatures from 340° to 540° K. Both precleaned mating surfaces and surfaces coated with special thermal grease according to General Electric specifications were used.

Material properties studied in this program included: (1) emittance, (2) thermal conductivity, (3) specific heat, (4) creep strength, (5) tensile strength, and (6) thermal expansion.

At the start of the program, an analytical investigation of the influence of thermal strain on joint conductance was made. The purpose was to find out whether distortion due to thermal expansion would change the contact pressure around the fastener, thus affecting the contact thermal conductance characteristics. The design of experimental apparatus would also have to take into account any such deviations in order to obtain realistic information. Analysis showed that no such correction was necessary.

Details of the technical approach, conducting the test program, the test results and their interpretations are contained in the following sections of this report.

II. TECHNICAL DISCUSSION

A. JOINT THERMAL CONTACT CONDUCTANCE

A major obstacle in theoretical analysis of the thermal performance of a spacecraft or the experimental modeling of such has been the lack of knowledge of thermal contact conductance of mechanical joints having an interface between the surfaces of contact. The resistance to heat flow through a mechanical joint depends on a number of parameters such as the thermal conductivity and the hardness of the materials, the surface conditions in both microscopic and macroscopic ways, the environment, the properties of the medium between the surfaces, the pressure, the way the surfaces are held together and the heat flux through the joint. In a bolted joint, it is further complicated by the uncertainty about the pressure produced by torquing.

Every one of these parameters will have to be dealt with in a general treatment. To meet the objective of this program, however, a number of simplifications can be applied to facilitate the study. The surface conditions can be closely matched by using the same machine finish as was used on the prototype, by using identical materials and fastening devices, and by applying the identical torques used on the prototype. In other words, a theoretically identical joint was made for the study.

For application to the thermal scale-model experiment (Task 4.1.a), the conditions were changed from those of the thermal contact conductance evaluation. To meet the criteria on thermal scaling with model temperatures the same as the prototype temperatures at homologous points, a material with a thermal conductivity different from that of the prototype has to be used for the model (Ref. 1). The area of contact is reduced in scale and different material properties are involved. One theoretically simple way, but difficult practically, is to make a scaled-down joint of the desired material and fastener, using some reproducible technique which will give the model the same thermal conductance as the prototype. Gabron, et al., used the first approach in the half-scale Mariner-Mars satellite modeling (Ref. 2). Another way is to establish a valid scaling law and then use this law to design the reduced model. This second approach was used in this program because of the difficulties involved in instrumenting and measuring thermal performance of extremely small scaled models.

Heat transfer through the metallic joint consisted of:

(1) Conduction through metallic contacts between the two surfaces

(2) Convection through fluid left between cavities on both sur-
faces

(3) Radiation.

For space applications where the environment is practically a vacuum,
convection by fluid is extremely small. It was found that below a pres-
sure of 10 microns of mercury, the convective contribution to contact
thermal conductance is negligible (Ref. 3). This was also confirmed
in this investigation. Since the temperature difference across the
interface is not large, generally from fractions of a degree to a few
degrees Kelvin, radiation heat transfer is also negligible. Thus, the
only heat transfer mode to be considered in this case is the conduction
through metallic contacts.

Contact thermal conductance of a mechanical joint in a vacuum
environment with no intermediate medium consists of metallic conduc-
tion through numerous microscopic high spots if the surfaces are
perfectly plane. For ordinary plane surfaces, there exists macro-
scopic irregularities or waviness which prevents the portions of the
microscopic high spots from contacting the other surface. Each of
these two phenomena has to be treated independently. If the surfaces
in contact are reasonably flat, the microscopic phenomenon may be
the predominant one. If the surfaces are rough and wavy, such as un-
machined surfaces, it may be the other way around. Most treatise on
this subject have been confined to the microscopic phenomenon. The
macroscopic phenomenon was treated by Clausing and Chao (Ref. 3)
in a doctoral dissertation at the University of Illinois.

An analytical treatise made by Hultberg (Ref. 4) assumed a linearly
decreasing distribution function, from the center toward the periphery,
of the thermal conductance of a bolted joint. The relation is represented
by the equation

$$\left[\bar{h} = h_o \quad 1 - c \left(\frac{r}{a} \right) \right] \tag{1}$$

where h_o is the maximum conductance at the edge of the bolt, a the
outer radius of the joint, r the radius and c the slope of the linear
variation. This approach sounds reasonable for rigid plane surfaces
with microscopic thermal constriction dominating. In a more rigorous
treatise of metallic plates held together by a bolt, each side of the
joint may be considered as a prismatic beam with a concentrated load
resting on an elastic foundation. Thus, the deflection of the plate at
distance x from the load application point may be given as (Ref. 5):

$$y = \frac{F\beta}{2k} e^{-\beta x} (\cos \beta x + \sin \beta x) \tag{2}$$

where

$$k = \frac{EI}{y} \frac{d^4y}{dx^4}, \quad \beta = 4\sqrt{\frac{K}{4EI}}$$

and F is the clamping or bolting load, E the modulus of elasticity, and
I the moment of inertia of the plate section. Equation 2 assumes a
wave form with gradually decreasing amplitude and becomes negative
a certain distance from the center. This solution would partially
justify the results of an experimental investigation by Aron (Ref. 6).
In Aron's experiment, it was found that the contact pressure varies
from a minimum at the bolt hole edge to a maximum between the bolt
head and the nut. The maximum pressure then declines to zero at a
distance (from the edges of the bolt head and nut) of 1.7 times the
thickness of the individual sheets of metal being held together. Beyond
this radius, the two sheets of metal tend to separate by a microscopic
amount.

Experimental investigation of thermal conductance of bolted joints
has been done by investigators at Douglas Aircraft Company (Ref. 7),
Arthur D. Little Company (Ref. 2) and others. Most of these were
measurements of thermal conductances of given design and under
given conditions. Scaling of thermal conductance of bolted joints has
been tried by Gabron, et al. (Ref. 2). To the best of our knowledge,
no published reports about experimental thermal scaling of bolted joints
are available at present.

B. MATERIAL PROPERTIES

The thermal and mechanical properties of alloy ZH62A at room
temperatures are listed in the Metals Handbook. For information of
material properties at temperatures close to the melting point, about
630° K, practically nothing is available. This is partly because
this alloy is generally used in the low or medium temperature range
up to 450° K and partly because the measurement of properties in the
higher temperature range is very difficult. The accuracy in the tem-
perature range close to its melting point is very inferior to that at
lower temperatures due to the possible change of phase or state of
portions of the alloy. Information about these materials will be
required for thermal and dynamical analyses.

Blank

III. TEST PROGRAM

A. JOINT THERMAL CONDUCTANCE TEST

1. Test Facility

The test facility used consisted of a spherical vacuum chamber equipped with mechanical and diffusion pumping systems. Accurate thermocouple readout was made using a Minneapolis Honeywell Model 2745 potentiometer referenced to an ice bath in conjunction with a selector switch made especially for thermocouple applications. Power for heating the test specimen was provided by a Model RVC 36-5M d-c power supply whose output voltage regulation under load is 0.01%. A multiple range d-c voltmeter plus a 50-mv meter connected across a five-ampere shunt was used to measure the electrical input to the specimen heating element. A picture of this setup can be seen in Fig. 1.

2. Test Models

Five joint specimens were tested. Three were representative of typical joint configurations existing in the structure of the Nimbus B satellite. They were made in two halves which were bolted or riveted together. Three of these were full size with the halves made of different metals, namely 2024-T4 aluminum and ZH62A magnesium. The other two were made of 304 CRES, one full size and the other half size for the thermal scaling study. The mating surfaces of all specimens were carefully machined to the same surface roughness or finish in an effort to duplicate that which exists in the actual vehicle. This finish was No. 125 as designated by the GE specification. These specimens, fully instrumented, are pictured in Fig. 2.

Heat meters made of round bars of Armco iron were used, one on each side of the test specimen. The input meter made of one-inch diameter stock had an electric cartridge heater brazed into one end and the other end threaded to receive the test specimen. In between, three calibrated thermocouples were installed in locations exactly one inch apart as measured along the longitudinal axis. The output meter made of half-inch stock had one end welded into a water-cooled heat sink and the other end threaded for attachment to the test specimen. It also contained three calibrated thermocouples installed in a like manner. The construction and use of these heat meters are clearly illustrated in Fig. 3.

3. Instrumentation

Each specimen was instrumented with chromel-alumel thermocouples. Except for Specimen 4, the following procedure was used
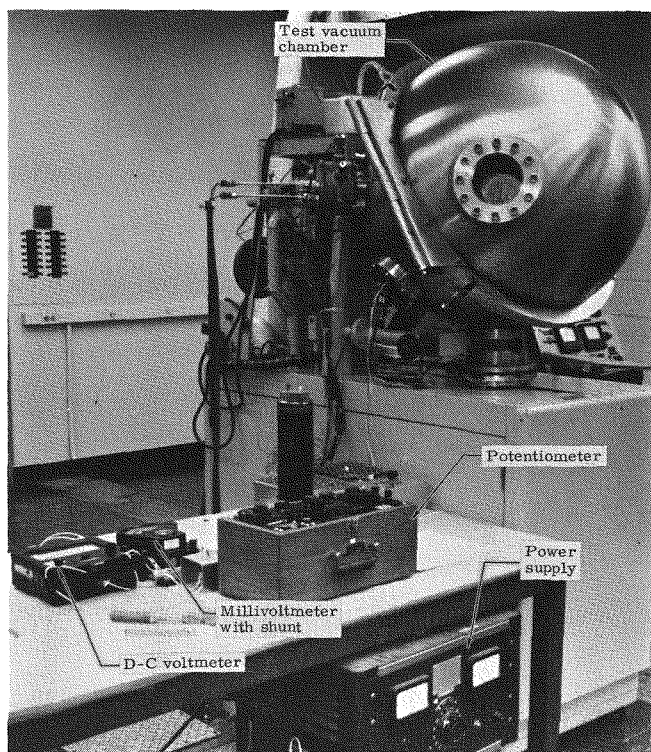
Fig. 1. Joint Thermal Conductance
Test Equipment
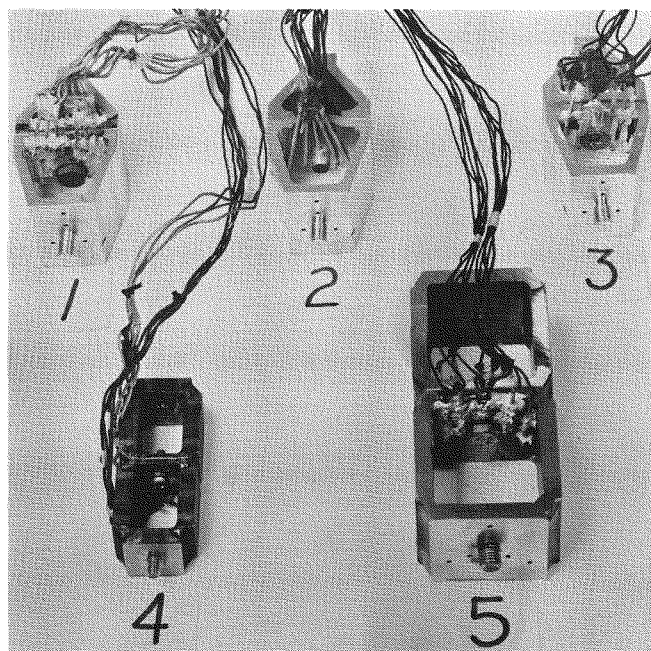
Fig. 2. Joint Thermal Conductance
Test Specimens
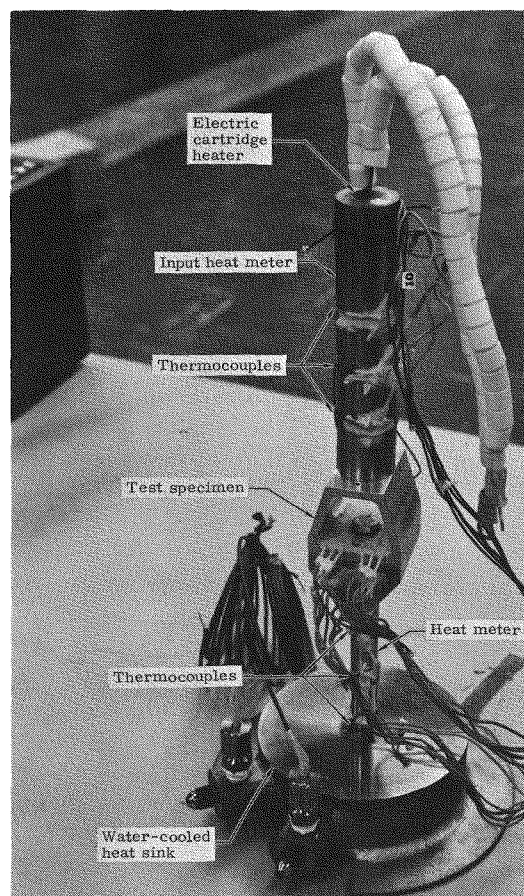
Fig. 3. Test Specimen and Heat
Meters on Test Fixture

for thermocouple installation. Holes (1.58 mm in diameter) were drilled from the opposite side to a distance of 0.50 mm from the mating surfaces. These holes fell directly opposite one another in each half of the specimen. Sections of two-hole ceramic insulating tube strung on the wire back of the junction were made slightly shorter than the depth of the hole. With this tube held tightly in the hole, the edge was peened over, thus causing the thermocouple junction to be held firmly against the metal at the bottom of the hole. Short pieces of ceramic tube, held in place with dabs of Saueriesen 31, were used for electrical insulation to avoid the possibility of the teflon coating on the wire breaking down at higher temperatures and shorting out the thermocouple. In the case of Specimen 4, the thermocouples were simply spot welded in place on the side opposite the mating surfaces. The number of thermocouples, their exact location plus details of the peening operation are more fully explained by Fig. 4. Installation of the thermocouples in the Armco iron heat meters was done in the same manner but at a uniform hole depth of 6.35 mm.

The thermocouples installed in both heat meters and Specimens 1 and 5 were calibrated before installation. Those in Specimens 2, 3 and 4, though not calibrated, were fabricated in the same manner and from the same spool of premium grade wire as the others.

4. Test Procedure

A series of 52 tests considering the following variables was completed.

(1) Joint temperatures ranging from 340° to 566° K

(2) Type of metals comprising the joint

(3) Type of fastening: whether hexagonal head, countersunk bolt or riveted

(4) Difference in bolt torque

(5) With or without heat-conducting grease between the mating surfaces

(6) Change in chamber pressure.

A listing of all the test runs made, classified according to these variables, is given in Table 1. A silicon grease-silver powder mixture made in accordance with General Electric Specification 171A4157 was used in the joint and was so noted. Prior to assembly of the specimen halves, all surfaces, particularly the mating surfaces, were thoroughly cleaned and rinsed with acetone. The halves were then

B

2024-T3 Al — — ZH62A Mg

Thermocouple locations
in both halves of test
specimen

Ceramic tubing
peened into place

Thermocouple
tight against
metal

0.020 in.

Thermocouple leads

Mating surface

B

1.625 in.

D'

D'

5 4

7

6

8

9

1.625 in.

B-B

D-D
D'-D'

Typical Specimens Nos. 1 to 3
(Al--ZH62A)

A

A

Specimen No. 4
(304 CRES)

C

C

Specimen No. 5
(304 CRES)

1.671 in.

D

D

5 4

7

6

8

9

1.593 in.

Thermocouple locations
in both halves of test
specimen

C-C

0.875 in.

0.970 in.

Thermocouples
spot welded to
opposite surface
(both halves of
specimen)

A-A

Fig. 4. Joint Conductance Specimens showing Thermocouple Locations

TABLE 1

Test Data (°F) from Thermocouples

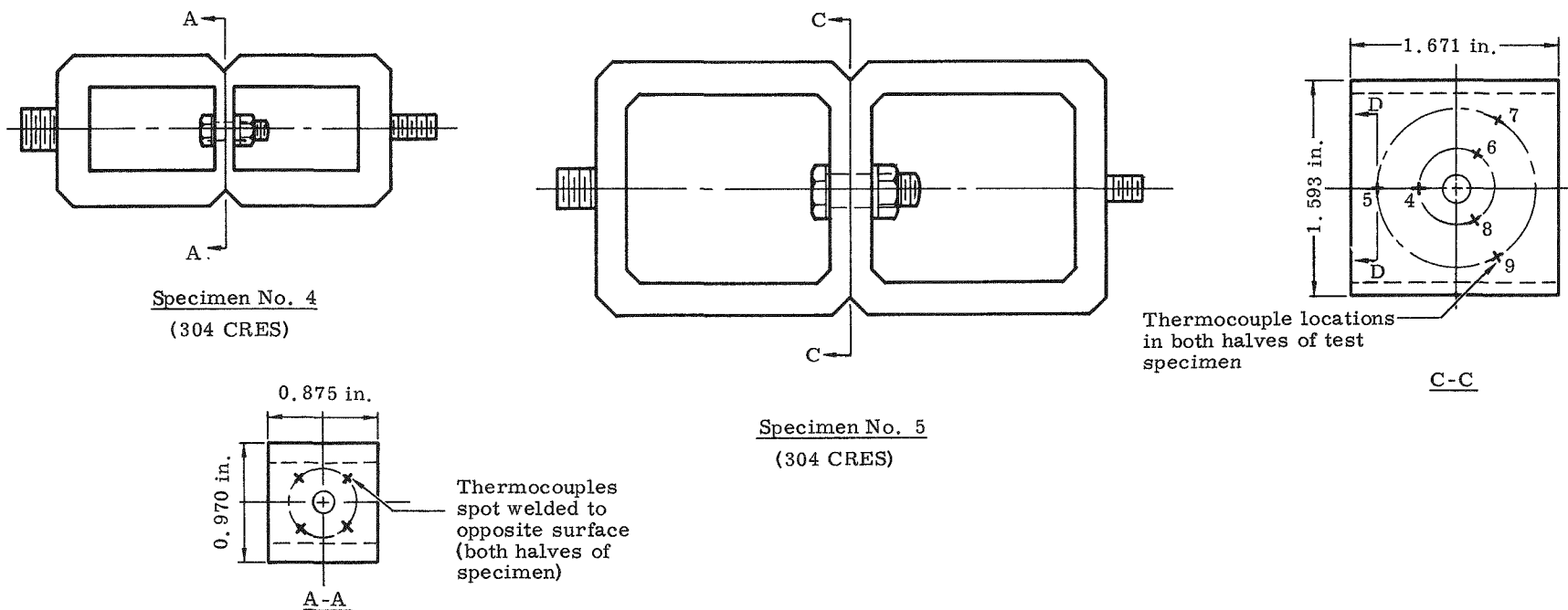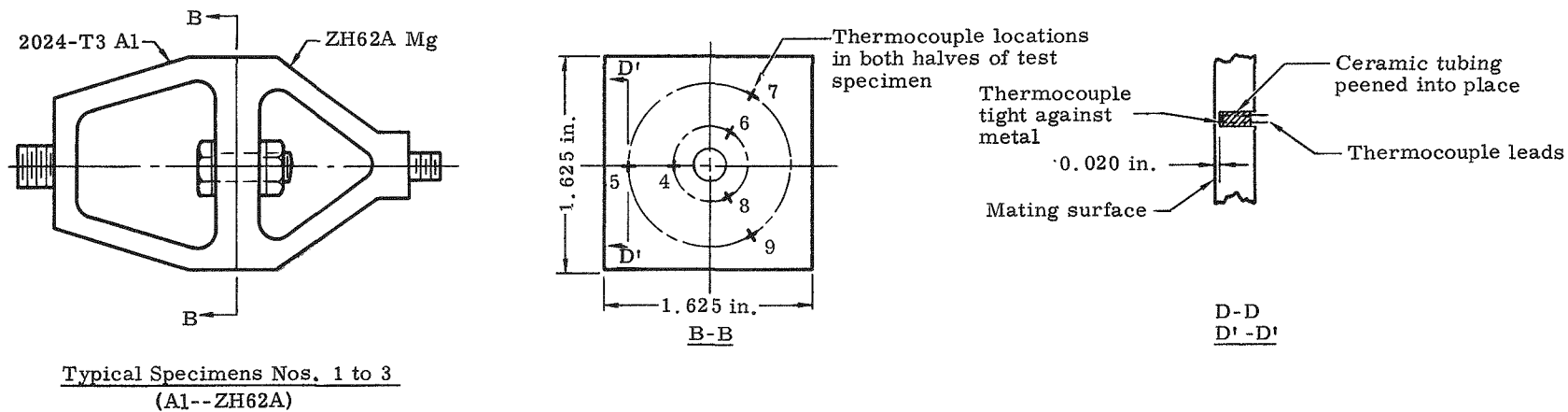| Test No.	Spec No.	Input Heat Meter			Hot Half of Specimen						Cold Half of Specimen						Output Heat Meter		
		1	2	3	*4	5	6	7	8	9	*10	11	12	13	14	15	16	17	18
1	1	714.0	670	622.5	531.9	534.1	531.89	537.87	530.35	537.62	521.3	520.63	527.1	518.14	527.13	NG			
2	1	463.33	439.05	415.91	340.01	342.2	340.2	340.07	340.05	344.21	331.14	335.4	338.37	331.38	332.82	NG	271.71	200.16	134.4
3	1	323.14	308.57	294.32	245.49	247.20	245.98	249.36	246.11	249.43	242.18	243.84	245.57	241.06	244.90	NG	203.3	156.5	113.2
4	1	182.7	177	172	151	150.8	150.8	152.2	150.9	152.2	149.1	149	150	149.1	149	NG	129.9	110.9	92.3
5	1	177	171.8	166.2	144.5	145	145.7	146.9	145.1	146.2	142.3	142.8	143.7	141.5	142.3	NG	123	104.2	85.1
6	1	330.51	315.57	300.85	248.40	250.28	248.8	252.41	248.71	251.88	240.26	245.78	247.76	242.23	246.71	NG	203.2	155.3	111
7	1	469.23	444.51	421.97	344.15	346.08	344.41	349.04	343.71	348.4	332.28	338.69	339.26	334.35	340.86	NG	272.95	201.48	135.9
8	1	683	643	605.1	506.23	508.77	506.73	512.09	505	511.84	493.13	495.7	496.4	490.34	499.46	NG	393.99	279.13	169.1
9	1	198.7	192	186	163.5	163.87	163.25	165.3	163.2	165.37	156.18	158.76	159.26	156.88	158.98	NG	133.5	113.5	94.2
10	1	190.7	183.9	178.1	157.38	157.68	157.11	158.86	157.22	158.89	150.62	152.1	153.04	150.78	152.44	NG	129.8	111	93.2
11	1	345.56	330.62	315.8	264.74	266.26	264.07	268.37	264.82	268.37	255.59	258.6	264.42	255.5	259.2	NG	210.5	166.3	123.8
12	1	365.62	350.64	335.35	279.69	282.16	279.44	284.2	279.7	284	270.28	273.74	274.87	270.02	274.75	NG	221.2	172.6	127.3
13	1	491.29	467.26	445	366.82	368.68	366.73	371.39	366.5	371.68	356.84	358.51	354.99	355	361.2	NG	282.62	212.42	147.2
14	1	479.8	456.6	434.77	352.65	354.05	352.06	356.31	351.57	356.6	342.52	344.10	341.72	340	346.14	NG	271.5	204.38	142.2
15	1	653.1	623	582.56	490.14	491.94	490.58	495.28	489.32	495.74	479.54	478.85	476.97	475.45	483.09	NG	375.8	274.04	178
16	1	670.5	633.1	599.04	513.44	515.06	514.42	518.6	513.14	519.74	503.64	501.54	500.61	497.31	505.76	NG	393.75	286.25	184.55
17	1	170	164.7	159.2	148.7	148.38	148.21	149.02	148.62	148.62	148.48	148.48	146.76	148.70	148.7	NG	130.1	110.8	92.5
18	1	301.98	NG	275.78	248.65	248.55	247.85	250.05	248.9	249.67	248.69	248.52	247.6	248.4	248.3	NG	205.58	159.9	116.6
19	1	440.71	417.71	396.33	352.82	352.85	351.96	353.08	352.98	353.94	352.61	352.65	351.59	351.83	352.53	NG	284.95	210.37	148.7
20	1	662.8	625	590	517.6	517.63	518.4	518.38	516.64	518.35	515.26	515.75	514.12	512.09	515.06	NG	411.82	293.8	182.3
21	2	219.52	213.71	208.16	172.74	172.66	171.15	171.74	170.9	171.12	NG	165.2	160.1	166.77	167.37	166.45	138.2	117.7	103.6
22	2	587.85	567.37	546.7	441.5	441.7	438.7	438.6	437	439	NG	422.5	404.3	426.1	426.4	424.8	325.97	255.65	205.45
23	2	753.2	718.4	687.75	552.6	552.6	549.5	550.2	548.8	550.7	NG	528.1	506.2	533.9	535.2	532.7	400.74	310.43	244.4
24	2	730.3	695.4	664.7	526	526	522.2	522.2	520.5	520.2	NG	501.2	473	504	504.5	501.2	364.5	269.3	200.5
25	3	172.2	167.1	162.2	148.8	148.7	148.2	150.8	150.6	150	147.6	147.6	147.4	146.1	146	146.3	128.4	110.9	94.2
26	3	305	293	280.8	249.02	249.64	248.31	253	252.84	251.8	246.21	246.88	246.88	243	243.1	243.65	201.8	157.8	116.9
27	3	421.98	402.2	383.6	338.46	340.03	338.56	344.28	344.04	342.87	335.21	336.42	336.3	331.4	331.2	331.97	266.72	200.16	139.3
28	3	632.5	597.33	566.4	500.96	503.59	501.8	508.32	507.72	506.16	496.02	499.02	494.46	490.02	490.86	492.06	384.78	278	177.2
29	3	161.8	157.5	152.6	141.52	141.26	140.26	141.88	141.88	141.46	141.32	141.32	141.09	141.09	141.18	141.09	124.7	107.8	90.9
30	3	303.5	290.58	277.67	251.88	251.55	249.92	252.45	252.15	251.75	250.92	250.7	250.92	250.67	250.95	250.95	205.8	160.8	118.5
31	3	432.55	413.07	392.94	351.35	351.58	349.98	352.6	352.28	351.15	350.5	350.87	350.47	349.72	350.45	350.72	281.85	209.66	143
32	3	630.7	595.39	563.29	500.96	502.4	501.2	503.36	502.88	501.2	499.52	500.72	497.84	498.8	499.76	500.24	397.3	286.64	182.36

TABLE 1 (continued)

Test No.	Spec No.	Input Heat Meter			Hot Half of Specimen						Cold Half of Specimen						Output Heat Meter		
		1	2	3	*4	5	6	7	8	9	*10	11	12	13	14	15	16	17	18
33	4	210.8	207.71	204.7	161.8	163	163.4	164.6			151	149.5	150.1	149.2			106	96.2	85.6
34	4	351.77	344.34	337.95	254.3	256.5	257	259.1			233.8	229.5	231.7	229.4			142.1	120.2	98.7
35	4	513.68	500.75	489.54	371.5	375.1	376.7	379.5			345.5	338.2	340.8	338			201.5	161	119.1
36	4	702.5	679.8	660.7	606	611.7	615.2	619			569.2	561.7	562.4	558.3			274.8	213	146.8
37	4	196.7	193.6	190.5	146.9	147.1	147.1	147.8			146.3	146.6	146.5	146.1			104.2	94.9	84.8
38	4	351.94	344.5	337.08	249	249.1	249.3	250			247.6	247.9	247.9	247.1			152	127.5	102.8
39	4	498.76	485.06	472.99	346.4	346.6	347.3	347.8			344	344.7	344.5	343.5			203.4	163.3	122
40	4	700	676.9	657.3	592.1	592.43	594.05	594.59			588.18	589.72	588.88	586.92			292.8	226.4	156.4
41	5	200.16	197.06	194.31	154.25	156.15	156.35	161.18	156.20	160.6	148	147.9	148.7	143.9	147.9	145.5	103	93.8	84.7
42	5	333.07	326.17	319.67	238.38	242.74	242.93	252.11	243.19	251.11	225.93	225.48	226.84	216.77	225.03	216.81	134	113.8	93.8
43	5	462.38	452.1	440.92	325.17	332.17	331.61	343.54	334.18	343.19	307.4	307.04	308.58	294.68	306.23	294.76	172.9	141.3	110
44	5	691	672.8	652.5	490.44	502.17	499.6	512.91	506.91	514.88	462.1	463.52	465.24	446.9	460.66	445.43	261.28	201.3	140
45	1	177.5	171.6	166.1	154.4	154.7	153.5	155.1	153.4	155.2	152.3	151.1	152.4	150.2	152	NG	130.2	110	90.3
46	1	319.15	305.45	291.24	261.15	262.92	260.82	265.1	261.15	264.95	257.72	256.16	258.72	254.14	257.9	NG	208.63	161.5	118
47	1	434.9	415.72	394.05	351.16	352.65	350.12	355.83	350.2	355.54	346.31	344.18	348.3	340.57	346.5	NG	259.18	203.87	137.5
48	1	670.1	632.1	594.45	525.23	527.15	524.44	530.69	522.44	525.79	517.83	514.35	520.14	506.75	517.86	NG	404.71	289.29	178.8
49	4	196.93	194.32	191.41	154.32	153.88	154.24	153.91			141.19	140.64	141.14	140.83			97.2	88	78.4
50	4	343.03	337.75	330.92	256.06	254.87	256.16	255.26			228.3	227.3	228.51	230.78			135.5	114.2	93.1
51	4	482.6	474.75	463.61	359.31	357.83	360.09	358.74			320.7	318.6	320.33	322.7			182.8	147.8	111
52	4	678.2	659	640.6	501.34	499.9	503.26	501.34			452.02	448.9	451.06	454.18			257.26	199.95	139.3

*T/C 4 was located directly opposite T/C 10, T/C 5 opposite T/C 11, etc.

fastened together, taking care that the mating surfaces did not twist or rub against each other during the process. A torque wrench calibrated for each specific experimental value was used on the nut to assure that the prescribed bolt tension limits were maintained. In the case of the riveted joint, standard riveting tools and processes were used for installing and heading the rivet. This was done in an effort to produce the conditions that would exist in the joint as the result of a typical assembly of this kind. After the input and output heat meters were in place, the heat sink was insulated with 10 layers of mylar-coated aluminum foil. A radiation shield consisting of four layers of highly polished and dimpled stainless steel sheet was placed over the entire test fixture. When power leads, water lines and thermocouples were hooked up and checked out, the chamber was closed and pump down started. Specimen 1, installed in the test fixture prior to being insulated, can be seen in Fig. 3. Figure 5 shows the same specimen completely installed in the chamber with the radiation shield in place.

By regulating the flow of water through the heat sink and the amount of power applied to the heater, various joint temperature levels were attained. Temperature data were taken every 10 minutes until stable thermal conditions were reached. The definition of stable thermal conditions established for purposes of this test was that point when the change in temperature indicated by Thermocouple 4 (located on the hot mating surface) did not vary more than 0.5° K in 15 minutes. When this condition was reached, all thermocouple outputs, heater power input and chamber pressure were recorded. A tabulated listing of the data obtained for each test run can be obtained from Table 2. Both Table 1 and Table 2 must be used together.

5. Data Presentation

    a. Data reduction procedure

The data obtained from the joint conductance thermal tests consisted of quasi-steady state temperatures at the following points:

    (1) Three locations spaced one inch apart in the direction of heat flow through the Armco iron heat meter (2.54 cm diameter) upstream of the contact point

    (2) Six (or four) different locations close to the interface on the hotter side of the contact plane

    (3) Six (or four) different locations close to the interface on the colder side of the contact plane

    (4) Three locations spaced one inch apart in the direction of heat flow through the Armco iron heat meter (1.27 cm diameter) downstream of the contact point.
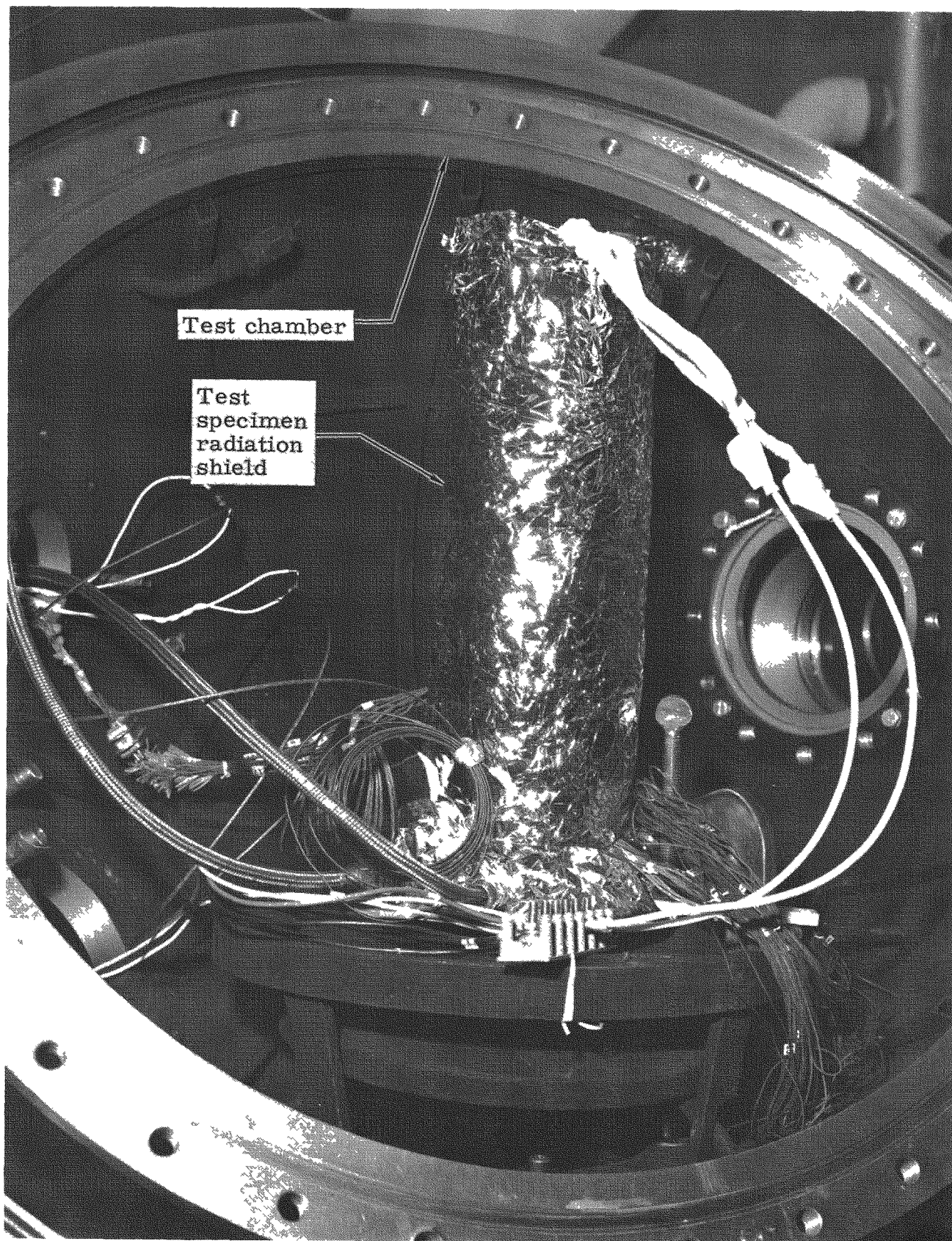
Fig. 5. Test Specimen Installed in Test Chamber

TABLE 2

Test Conditions and Results

Test No.	Specimen No	Material	Fastening	Torque (in-lb)	Greased	Chamber Pressure (torr)	Joint Temperature (°F)	Scale	Average Heat Rate (Btu/hr)	Joint Conductance (Btu/hr-ft²-°F)	Joint Conductance (watt/m²-°K)
1	1	ZH62A-Al	Hex bolt	55	No	1×10^{-2}	532	Full	73 45	350	1,985
2						1×10^{-2}	340		47 55	388	2,200
3						1×10^{-2}	245		31 80	522	2,960
4						1×10^{-2}	148		12 59	361	2,046
5						3×10^{-5}	145		13 16	245	1,390
6						3×10^{-5}	248		32 70	345	1,957
7						2×10^{5}	344		46 65	304	1,724
8				55		2×10^{-5}	506		71 05	304	1,724
9				40		$1 75 \times 10^{-5}$	164		14 52	136	772
10						1×10^{-2}	157		14 09	131	744
11						1×10^{-2}	265		31 30	193	1,095
12						1.75×10^{-5}	280		32 65	214	1,214
13						1×10^{-5}	367		45 92	243	1,380
14						1×10^{-2}	353		45 70	246	1,396
15						1×10^{-2}	490		64 00	275	1,560
16				40	No	1.5×10^{-5}	513		65 50	271	1,539
17				55	Yes	4×10^{-4}	149		13 10	1930	10,950
18						$1 6 \times 10^{-4}$	249		30 08	3280	18,600
19						$3 5 \times 10^{-5}$	353		46 65	5090	28,850
20	1		Hex bolt	55	Yes	$3 2 \times 10^{-5}$	518		69 40	1155	6,570
21	2		Rivet	--	No	1×10^{-2}	173		13 58	143	813
22						1×10^{-2}	442		41 85	161	915
23						1×10^{-2}	553		54 00	163	926
24	2		Rivet	-		1×10^{-5}	526		56 60	158	898
25	3		Counter-sunk bolt	55		$3 2 \times 10^{-5}$	149		12 01	244	1,385
26						2.6×10^{-5}	249		28 10	263	1,492
27						2.7×10^{-5}	338		41 50	297	1,685
28					No	$2 5 \times 10^{-5}$	501		61 90	306	1,735
29					Yes	9×10^{-5}	142		11 49	1560	8,870
30						5.5×10^{-5}	252		29 40	1430	8,130
31						4×10^{-5}	351		43 70	1775	10,070
32	3	ZH62A-Al	Counter-sunk bolt	55	Yes	$3 2 \times 10^{-5}$	501	Full	65.30	1410	8,020
33	4	304 CRES	Hex bolt	9 75	No	3.2×10^{-5}	162	1/2	7 20	92 6	525
34						$3 2 \times 10^{-5}$	254		14 43	95 5	542
35						3×10^{-4}	372		25 92	125	711
36					No	4×10^{-4}	606		39 42	134	762
37					Yes	$1 3 \times 10^{-4}$	147		7 14	1425	8,100
38						8×10^{-5}	249		16 66	1635	9,260
39						8×10^{-5}	346		26 75	1590	9,040
40	4	304 CRES		9 75	Yes	7×10^{5}	592	1/2	41 00	1425	8,100
41	5	347 CRES		55	No	2.8×10^{-4}	154	Full	6 72	35	199
42						$4 7 \times 10^{-5}$	238		14 44	35 4	201
43						4×10^{-5}	325		21 80	37 3	212
44	5	347 CRES				$2 5 \times 10^{-5}$	490		36 95	42 8	243
45	1	ZH62A-Al				3×10^{-4}	154		13 88	289	1,640
46						$1 4 \times 10^{-4}$	261		31 03	320	1,815
47						$2 2 \times 10^{-5}$	351		41 85	335	1,900
48	1	ZH62A-Al		55		2.2×10^{-5}	525	Full	70 00	360	2,044
49	4	304 CRES		9.75		$5 5 \times 10^{-5}$	154	1/2	6 75	87 1	494
50						$4 3 \times 10^{-5}$	256		14 92	94 8	538
51						2.5×10^{-5}	359		23 15	102	580
52	4	304 CRES	Hex bolt	9.75	No	$2 3 \times 10^{-5}$	501	1/2	35 25	120	682

In addition to these temperature measurements, test data included the chamber pressure and the heater voltage and current.

When reducing the data, the heat flow rate, q, is calculated as

$$q = (kA\Delta T)/x \tag{3}$$

where x is the meter length corresponding to the temperature rise or drop, ΔT.

From the six heat meter temperatures, four different values of the heat flow rate for each test were calculated. Due to progressive heat loss by radiation and residual gas conduction, the calculated heat flow rate normally showed a reduction from one heat meter section to the next. This occurred even though there was a radiation shield. However, since the contact joint is approximately centered between the various heat meter sections, it can be reasonably assumed that the heat flow rate through the joint is the arithmetical average of the four different rates calculated.

The thermal conductance of the joint is calculated as

$$h = q_{ave}/A_{ij} \Delta T_{ij} \tag{4}$$

where A is the surface area of the contact and T is the temperature drop across the joint.

The mean temperature difference across the contact interface, T_{ij}, is calculated by subtracting the average of six (or four) temperatures on the cold side of the interface from the average of six (or four) temperatures on the hot side of the interface.

b. Test results

The total number of tests conducted amounted to 52, using five different contact joints as described previously. Thermocouple readings from all tests are presented in Table 1. Test conditions and results of calculated thermal conductance for each condition are presented in Table 2. Figure 6 shows the thermal conductance of specimens with clean surfaces of contact, and Fig. 7 illustrates those with contacting surfaces coated with a special thermal grease impregnated with silver powder per General Electric Specification 171A4157.
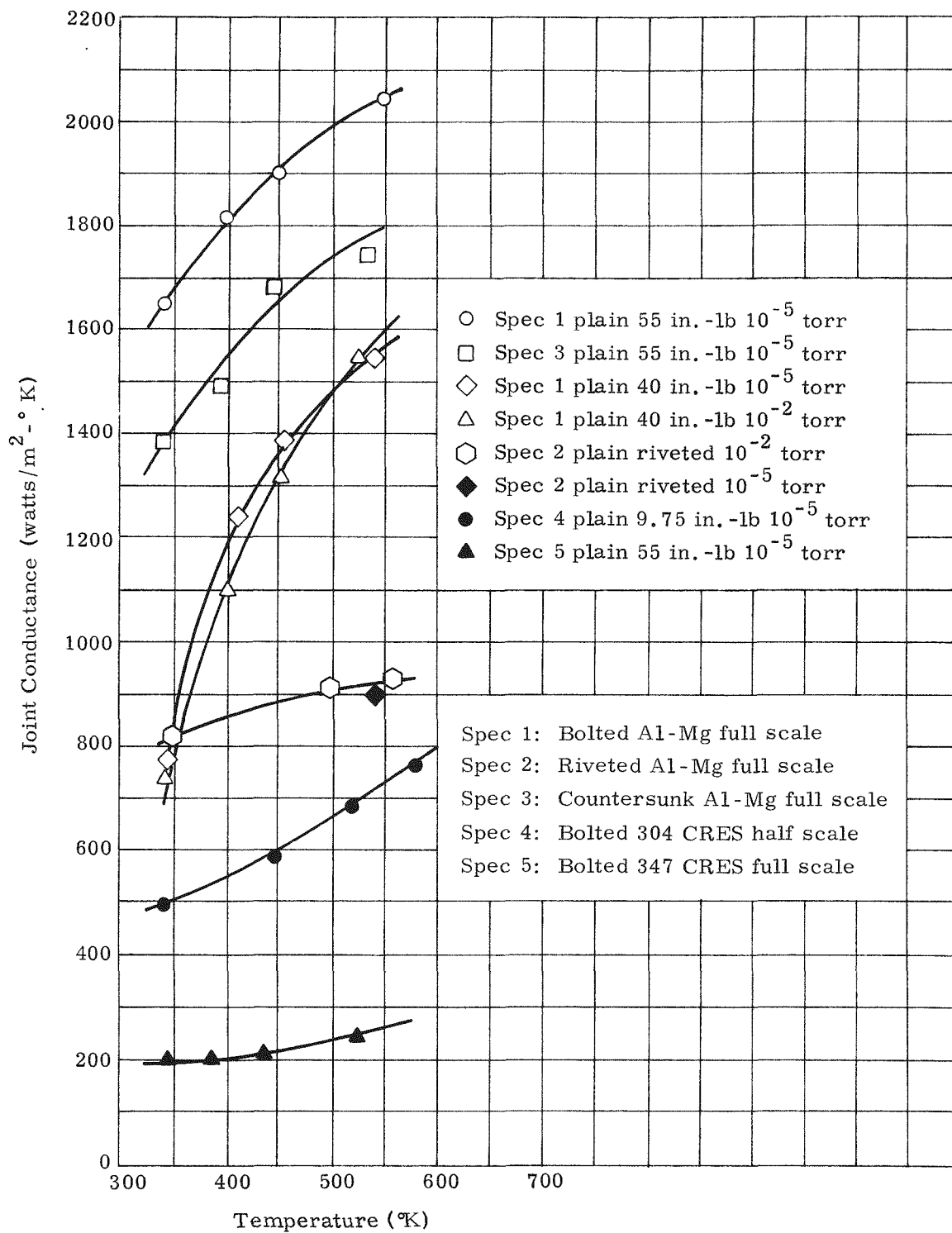
Joint Conductance (watts/m^2-°K)

2200

2000

1800

1600

1400

1200

1000

800

600

400

200

0

300   400   500   600   700

Temperature (°K)

O Spec 1 plain 55 in.-lb 10^{-5} torr
□ Spec 3 plain 55 in.-lb 10^{-5} torr
◇ Spec 1 plain 40 in.-lb 10^{-5} torr
△ Spec 1 plain 40 in.-lb 10^{-2} torr
⬡ Spec 2 plain riveted 10^{-2} torr
◆ Spec 2 plain riveted 10^{-5} torr
● Spec 4 plain 9.75 in.-lb 10^{-5} torr
▲ Spec 5 plain 55 in.-lb 10^{-5} torr

Spec 1: Bolted Al-Mg full scale
Spec 2: Riveted Al-Mg full scale
Spec 3: Countersunk Al-Mg full scale
Spec 4: Bolted 304 CRES half scale
Spec 5: Bolted 347 CRES full scale

Fig. 6. Joint Thermal Conductance Versus Temperature for Ungreased Joints
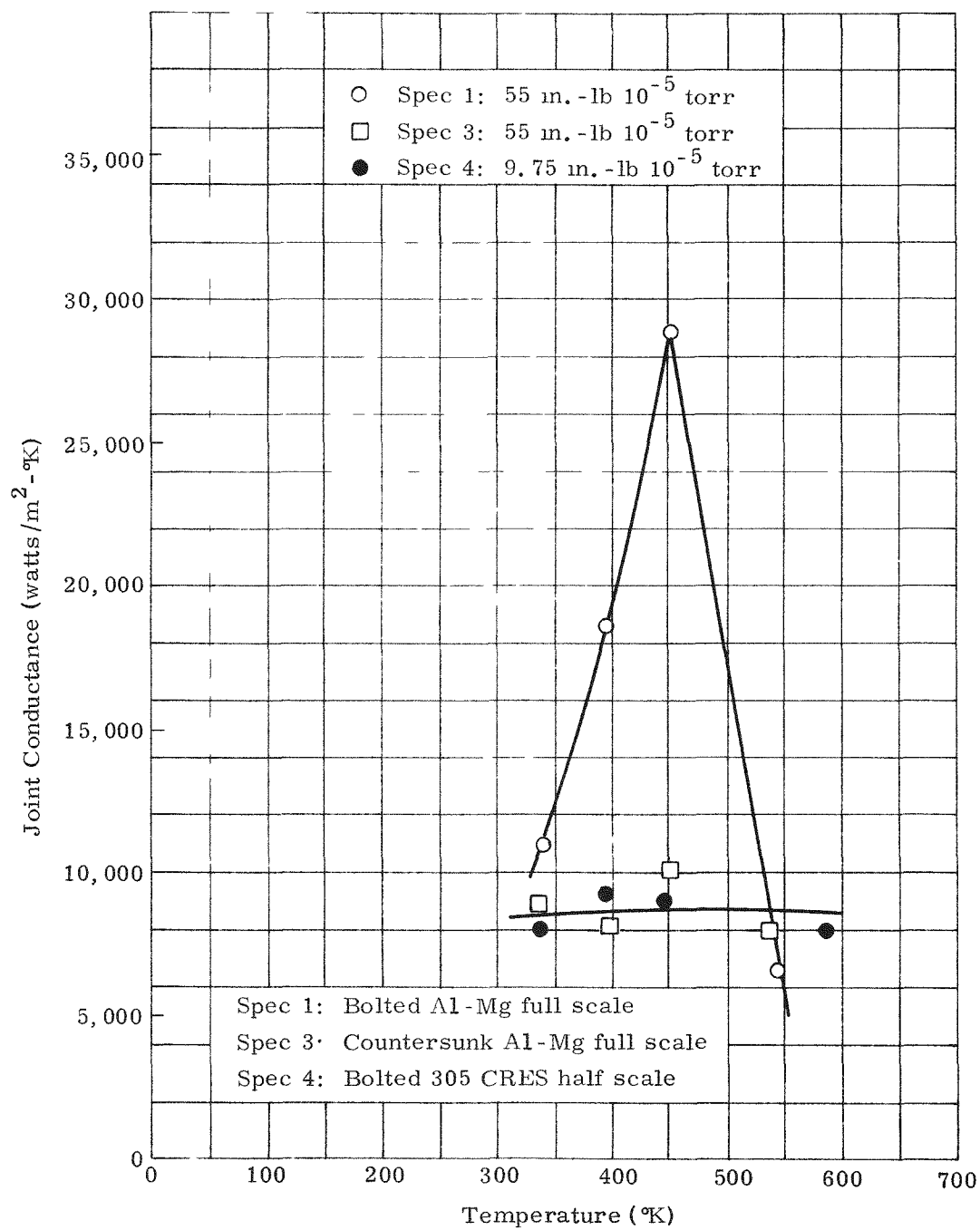
Fig. 7. Joint Thermal Conductance Versus Temperature for Greased Joints

B. THERMAL AND MECHANICAL PROPERTIES OF ZH62A ALLOY

1. Emissivity Measurement

Both the total hemispherical and normal emittances were determined. Since emittance is also dependent upon the conditions of the surface, each specimen surface was finished to match that specified for the Nimbus B structure.

The total hemispherical emittance was determined using the calorimetric test method at the Martin Test Facility. A hollow cylindrical test specimen whose interior was heated electrically was suspended by the power leads in the center of the evacuated and cooled test chamber. Figure 8 illustrates the test specimen and Fig. 9 shows the facility. The chamber pressure was maintained below 10^{-5} torr to keep the heat loss by means of gaseous convection at a negligible level. After the specimen had reached thermal equilibrium, its emittance was calculated from the known relationship between the electrical power dissipated, area and equilibrium temperature of the specimen. Suitable corrections were made for electrical resistance and thermal conductivity losses in the heater leads. Test results at two temperature levels are as follows:

Equilibrium Temperature (°K)	Emittance
554	0.111
672	0.116

The total normal emittance was determined through the use of a Gier-Dunkle reflectometer shown in Fig. 10, using a single beam mono-chromator. The test specimen was made of a flat disc of ZH62A alloy. The reflectance was measured in an integrating sphere for wave lengths from 0.295 to 2.7 microns in 2% increments of the Johnson curve. The sample was transferred to the heated cavity, and reflectance measurements were made at from 1.4 to 25 microns. The total normal emittance was then determined by integration of the reflectance curve for every 2% increment of the Planckian curve for distribution of energy of a black body at 610° and 700° K.

Next, the specimen was subjected to simulated use conditions for two hours. This consisted of placing it in a vacuum chamber at a 20-to 30-micron pressure level while holding the temperature of the specimen at 682° K. After this, the total normal emittance was again determined in the same manner as before. The calculated results of the total normal reflectance tests were as follows:
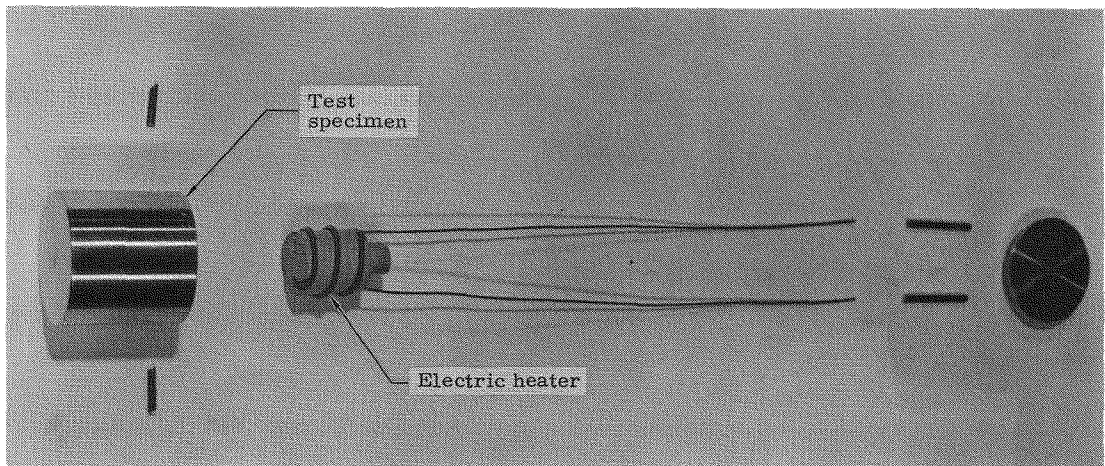
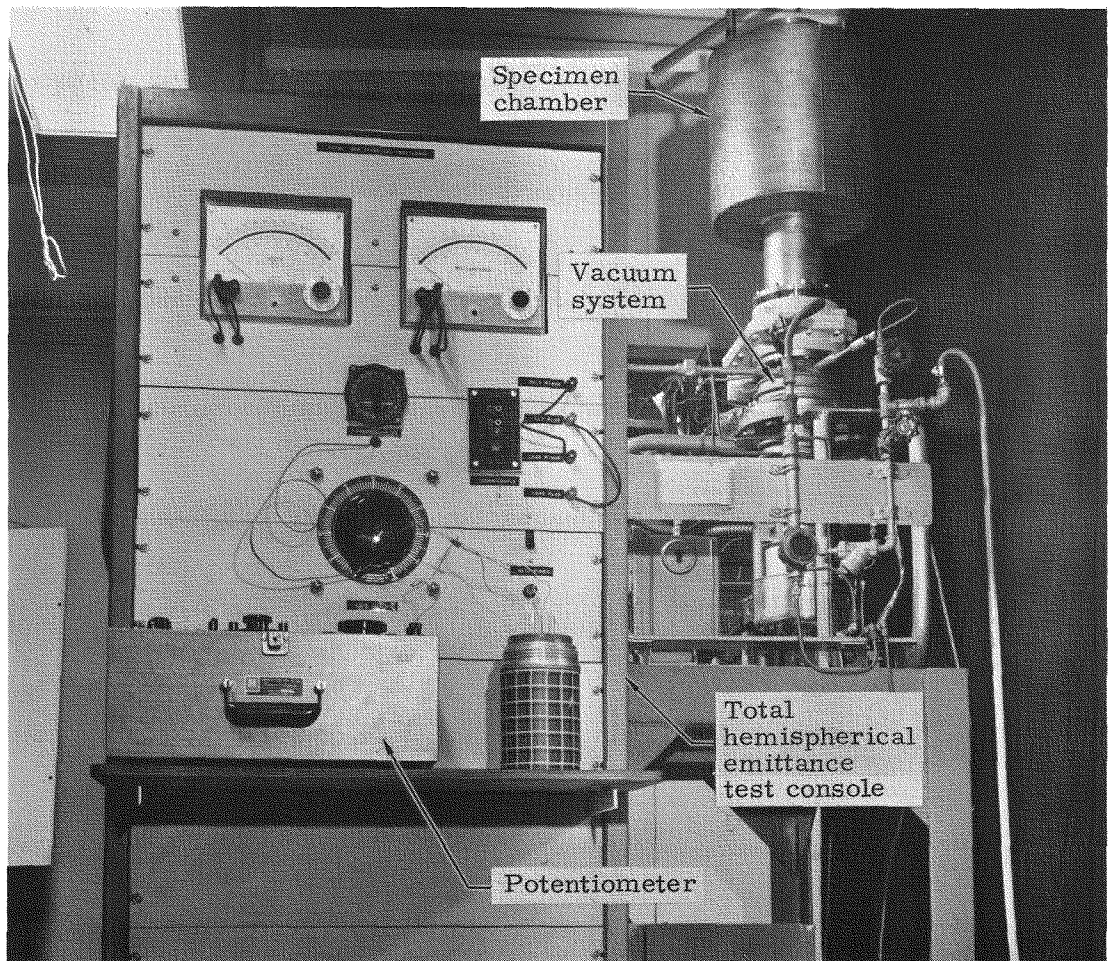Fig. 8. Test Specimen Used in Total Hemispherical Emittance Test

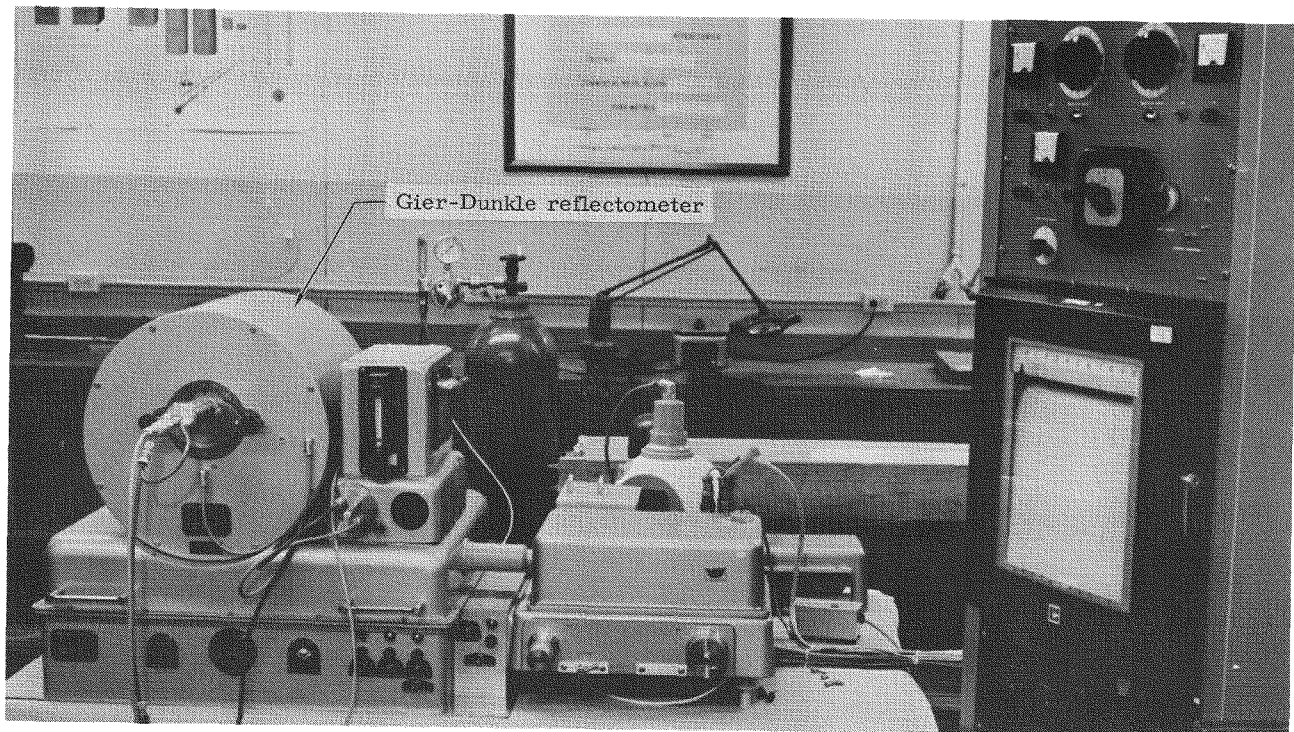Fig. 9. Test Facility Used for Total Hemispherical Emittance Test

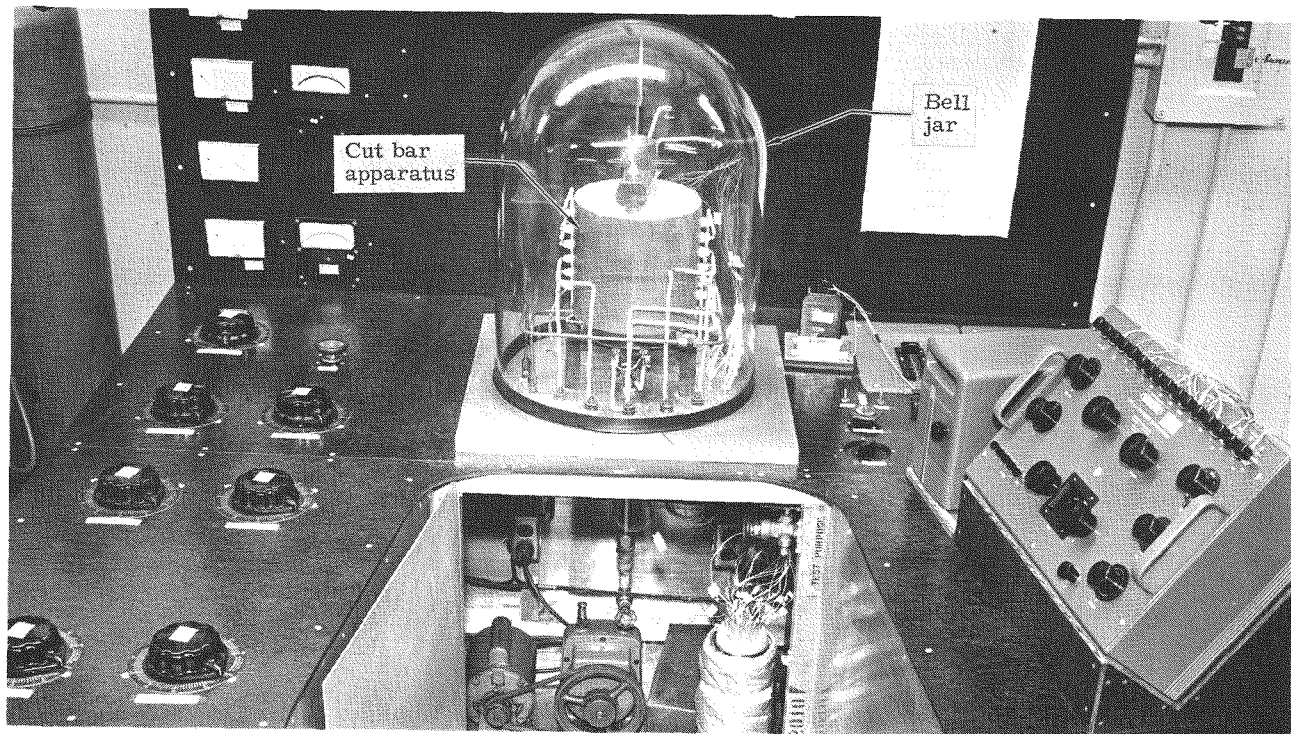Fig. 10. Test Facility Used for Spectral Reflectance Test

Fig. 11. Test Facility Used for Thermal Conductance Test

Temperature (°K)	E Original	E After Vacuum
610	0.080	0.081
700	0.089	0.091

2. Thermal Conductivity Measurement

Thermal conductivity measurements were made at temperatures ranging from 600° to 783° K in an inert argon atmosphere using the Martin cut bar apparatus pictured in Fig. 11. This equipment compares the known thermal conductivity of a standard material with that of the specimen being tested. The test specimen and standard, including a system of thermal guard zones, are stacked together in a manner which ensures that parallel isotherms exist in the stacks. The standard acts as a metering bar for determining the heat flux to which the specimen is subjected. The precise measurements required to determine the temperature gradient through the standard and test specimen are made with platinum-rhodium thermocouples which are accurate to 0.1° C. The conductivity of the specimen being tested is determined mathematically after the heat flow rate and temperature gradient through the material are known. The thermal conductivity of this material based on the results of this test is described by the curve in Fig. 12.

3. Specific Heat Measurements

An adiabatic drop calorimeter was used as the tool to determine the specific heat of the specimen material at temperatures ranging from 583° to 783° K. This apparatus consisted of a furnace, 3.8 centimeters in diameter and 51 centimeters long, connected to a calorimeter through a straight tube as pictured in Fig. 13. The furnace was purged with helium to minimize oxidation of the test specimen. The calorimeter containing a known mass of water is surrounded by a protective jacket which is maintained at the same temperature as the water. A special gate located at the top of the receiver prevents heat loss due to radiation during the dropping action.

For each temperature level of interest, the specimen is suspended in the furnace until steady state thermal conditions exist. The specimen is then dropped into the water of the calorimeter and left there until water and specimen reach the same temperature level. The specific heat is then calculated from the known values of specific heat, mass and temperature increase of the water, and the mass and temperature decrease of the specimen. The curve shown in Fig. 14 is the result of tests performed according to this procedure for the subject material.
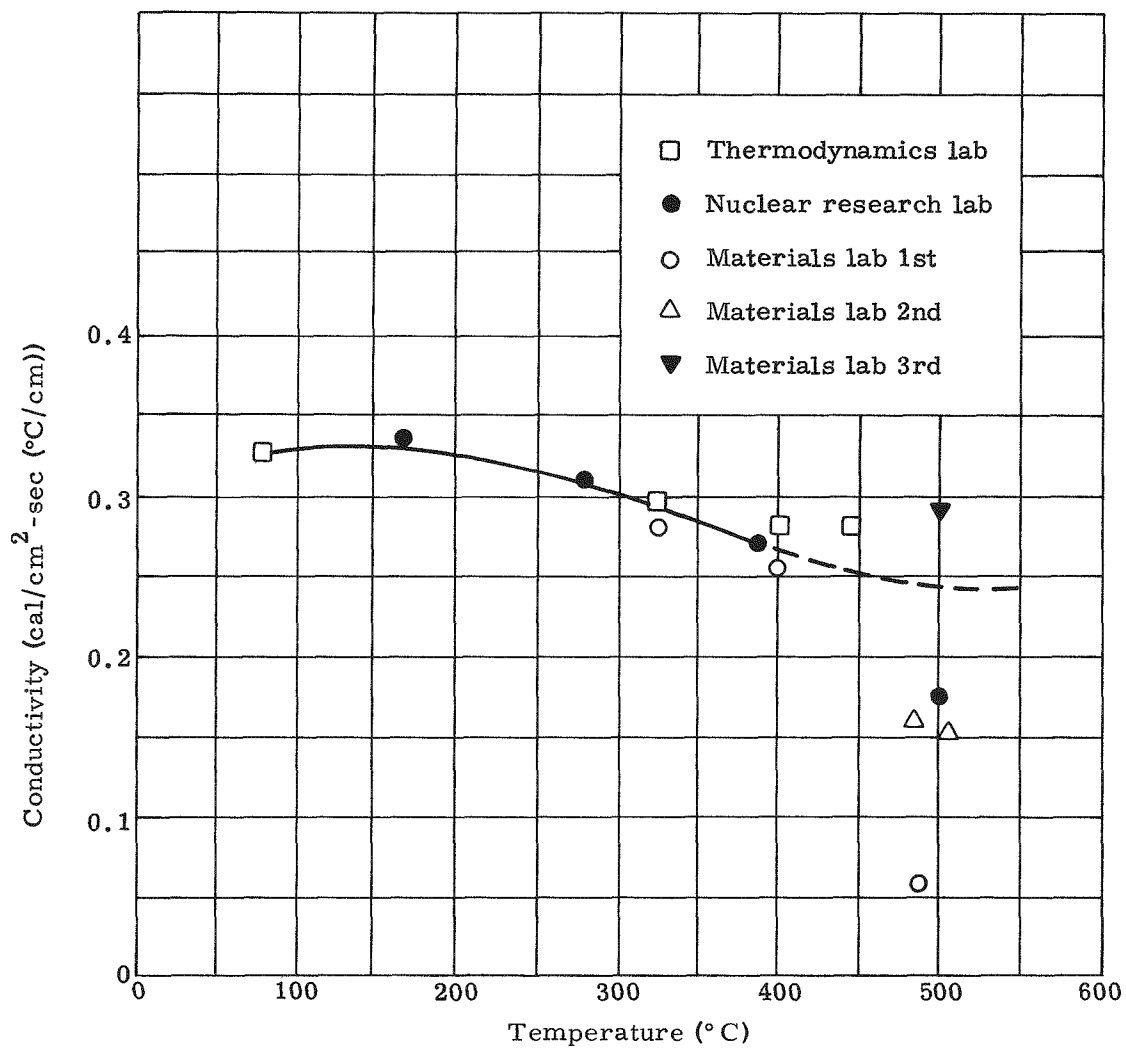
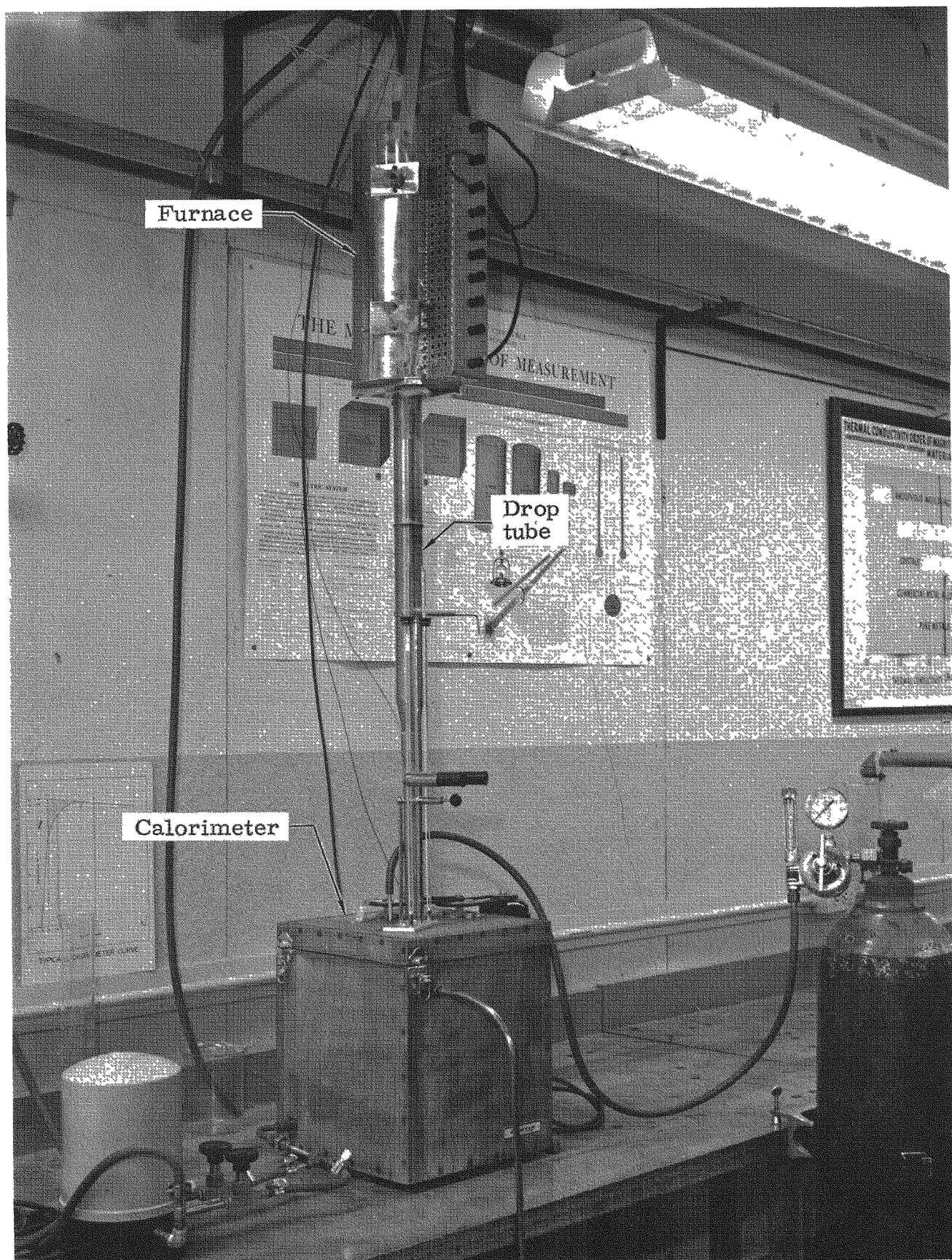Fig. 12. Thermal Conductivity of ZH62A Versus Temperature

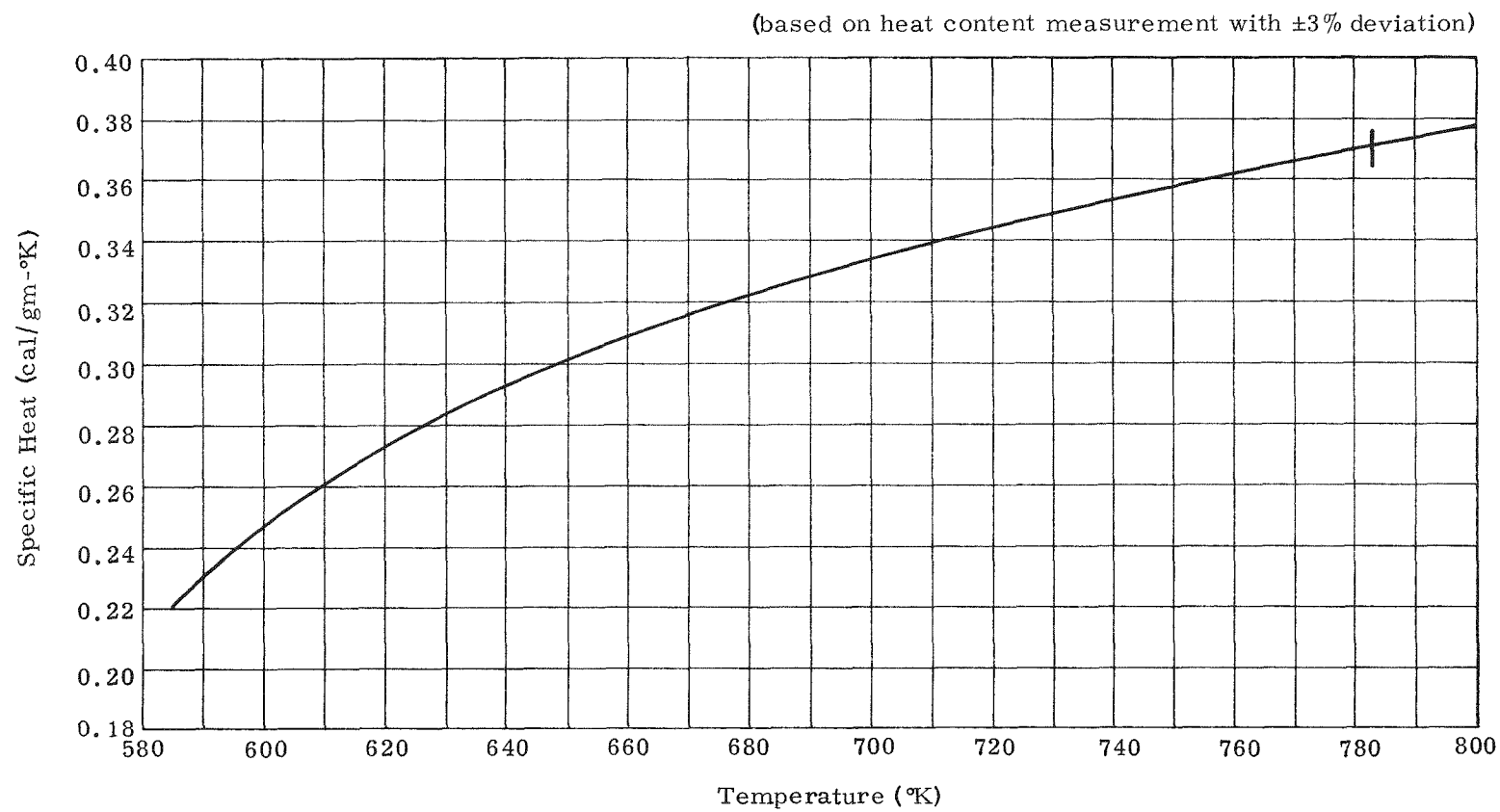Fig. 13.   Test Facility Used for Specific Heat Test--Drop Calorimeter

(based on heat content measurement with ±3% deviation)

Fig. 14.   Specific Heat, ZH62A Versus Temperature

4. Creep Measurements

Creep properties at specimen temperatures of 583°, 683°, and 783° K were measured using a Baldwin Lever creep testing machine (Fig. 15). This apparatus consists of a device for applying a load on the specimen, a furnace for maintaining the specimen at a precise elevated temperature and an extensometer with a recorder for measuring material deformation to an accuracy of 0.005 mm.

After installing a specimen in the machine, the furnace was purged with argon, the temperature brought to the desired level and the load applied. The temperature of each specimen was monitored by an attached chromel-alumel thermocouple. Each specimen was tested under load for three hours or until a failure occurred, whichever came first. The results of these tests are listed in tabular form in Table 3.

5. Tensile Properties

Yield and ultimate strength, elongation and tensile modulus were obtained for this material at 295° (room temperature), 583°, 683° and 783° K. These tests were performed using a 2270-kilogram PTE Universal test machine with a Marshall furnace attached as shown in Fig. 16. A separable extensometer with recorder was used to measure changes in the specimen length. Specimen temperature was monitored by a chromel-alumel thermocouple fastened to each specimen.

Each specimen was mounted in the machine surrounded by, but not touching, the Marshall furnace. During the heating period, the furnace was continually purged with an inert argon gas in order to preclude oxidation of the material specimen. Three specimens at each temperature were tested. The results of these tests are listed in tabular form in Table 4.

6. Thermal Expansion

Measurements of the thermal expansion of this material were made at 100° K intervals from 383° to 783° K using the quartz tube dilatometer shown in Fig. 17. Both dilatometer and specimen were placed in a Marshall furnace which was kept purged of air by argon gas to prevent oxidation of the test specimen. A chromel-alumel thermocouple embedded in the specimen was used to monitor its temperature. Figure 18 shows the results of this test.

Fig. 15. Test Facility Used for Creep Measurements

TABLE 3

Creep Test Results

| Specimen | Temperature (°K) | Stress (kg/cm^2) | Creep Strain (min) | | | Comments |
			One Hour	Two Hours	Three Hours	
M-13	583	352	0.0036	0.0055	0.0074	
M-14	583	422	0.0071	0.0144	0.0259	
M-15	583	421	0.0141	0.0378	0.0674 max, 2.5 hr	Specimen failed after 2.5 hours
M-16	683	253	0.0416	0.0540 max, 1.1 hr	--	Specimen failed after 1.1 hours
M-17	683	253	--	--	--	Creep rate exceeded capacity of machine to maintain lever arm level
M-18	683	206	0.0310	0.0695 max, 1.4 hr	--	Creep rate exceeded capacity of machine to maintain lever arm level
M-19	783	--	--	--	--	Failed in threads prior to loading
M-20	775	6.2	--	--	--	Failed in threads
M-21	755	6.2	--	--	--	Failed in threads
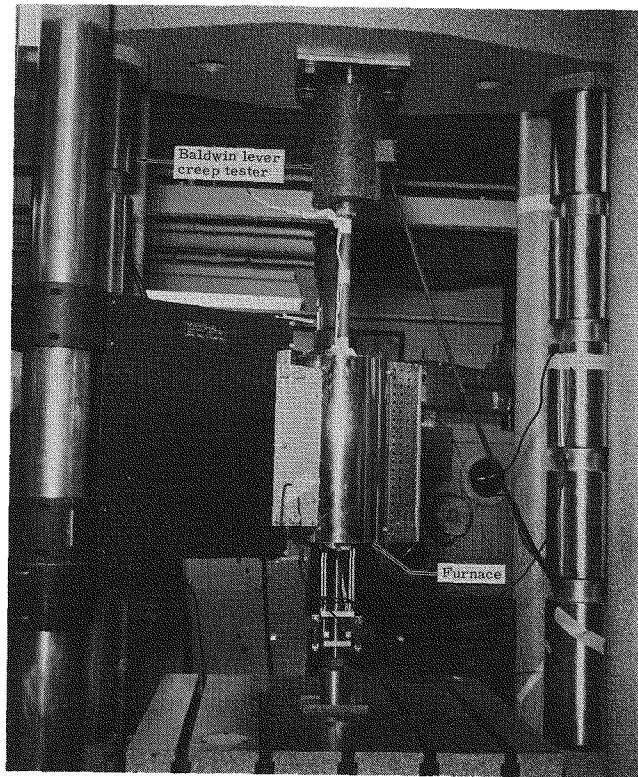
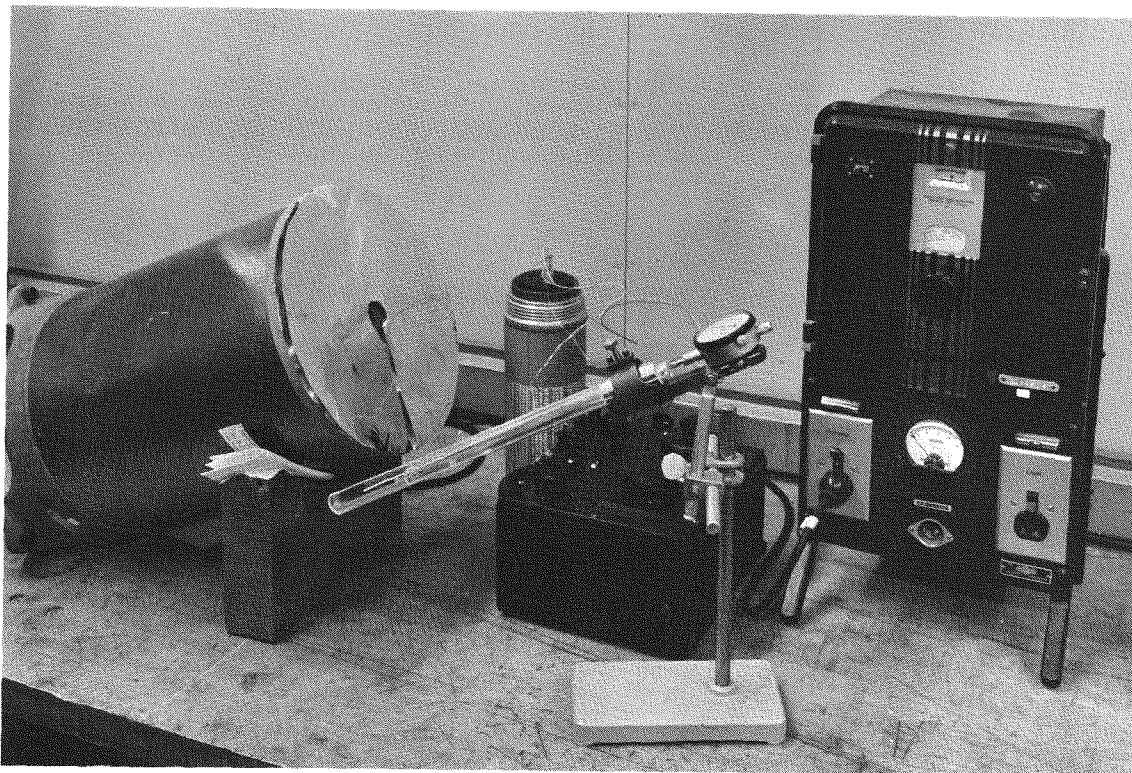Fig. 16.   Test Facility Used for Tensile Properties

Fig. 17.   Test Facility Used for Thermal Expansion Measurement

TABLE 4

Summary of Tensile Test Data

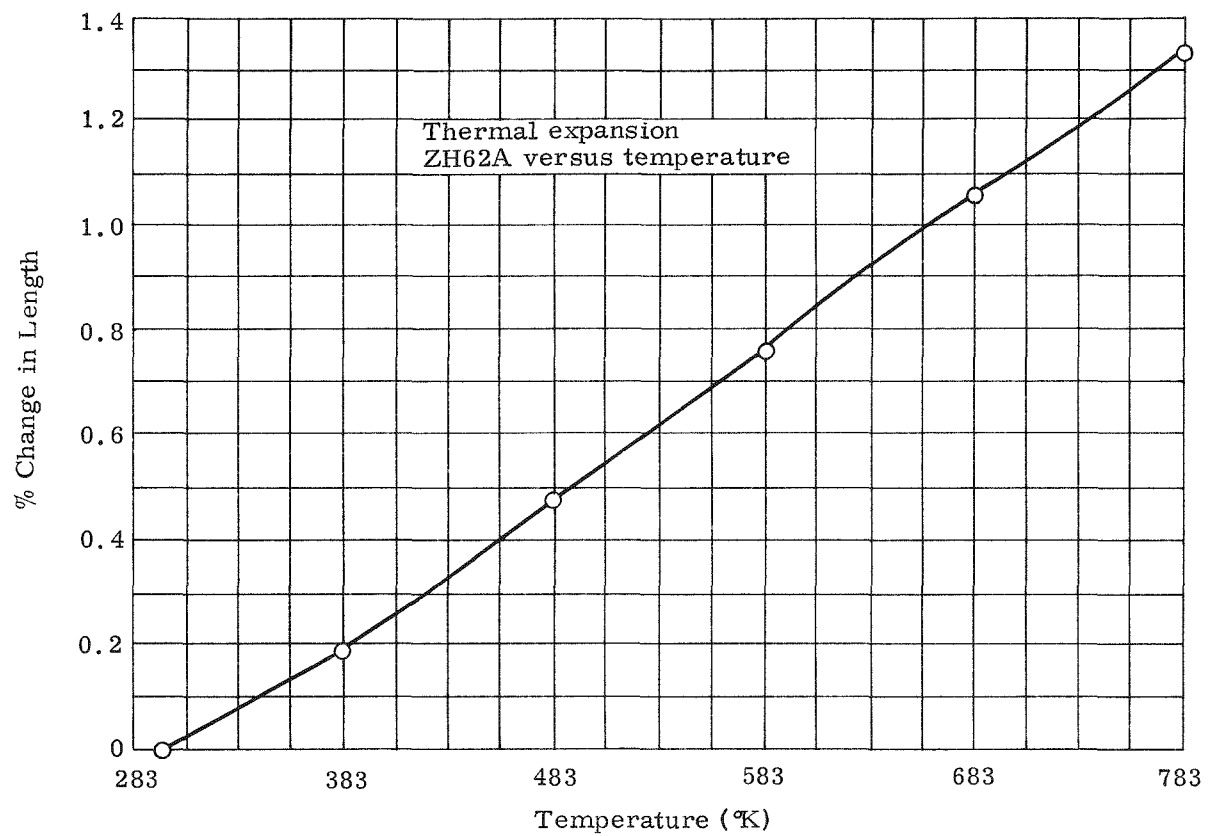| Sample No.	Area (in.^{2})	Yield Stress (psi)	Ultimate Stress (psi)	Elongation (%)	Modulus $\times 10^{-6}$ (psi)
Room Temperature					
M-1	0.2001	21,490	35,080	6.0	6.22
M-2	0.1999	22,010	37,120	7.0	6.04
M-3	0.2001	21,990	32,580	4.5	6.14
Temperature 583° K (589° F)					
M-4	0.2001	7,750	11,640	27.0	4.21
M-5	0.2001	7,900	11,120	38.0	4.16
M-6	0.2005	7,360	10,820	31.0	3.59
Temperature 683° K (769° F)					
M-7	0.1994	4,860	6,270	41.0	3.24
M-8	0.2001	4,750	5,470	21.0	2.69
M-9	0.2001	4,000	4,720	--	2.94
Temperature 783° K (949° F)					
M-10	0.2001	--	210	--	--
M-11	0.2001	--	115	--	--
M-12	0.2001	--	90	--	--

Fig. 18. Thermal Expansion, ZH62A Versus Temperature

Blank

IV. DISCUSSION OF RESULTS

A. JOINT THERMAL CONTACT CONDUCTANCE

Theoretical analysis of microscopic contact conductance (Refs. 3, 8, 9) indicated that under vacuum conditions conductance is directly proportional to the material conductivity and to the pressure applied to the contact surfaces, and inversely proportional to the micro hardness and surface roughness index. In analytical form, the microscopic contact thermal conductance may be expressed as (Ref. 2)

$$h = \frac{2K_{ij} P_a}{H\, a_{mi}} \tag{5}$$

where $K_{ij} = 2K_i \times K_j / (K_i + K_j)$ is the combined thermal conductivity when heterogeneous materials are used such as in the case of three of the five specimens tested, P_a is the contact pressure, H is the micro-hardness of the harder material and a_{mi} the radius of each microscopic contact area which is assumed to be circular. Test results of all un-greased specimens show a rising thermal conductance with temperature. For Specimens 1, 2 and 3 which consisted of pairs with 2024-T4 Al contacting ZH62A Mg, and fastened by a steel bolt, this is most likely caused by an increase in contact pressure, P_a. This increase is due to the lower value of the coefficient of thermal expansion of the steel than those of the aluminum and magnesium alloys, since the combined conductivity of the magnesium and aluminum alloys does not vary much with temperature. For the two steel specimens fastened by steel bolts, the slight rise in conductance with temperature is probably due to the rising thermal conductivity, K_{ij}, of the material with temperature.

The top curve in Fig. 6 shows some peculiarity of reduced thermal conductance above 250° F. The only explanation of this is that the four tests which resulted in this curve were conducted at the outset of the program, prior to gaining sufficient experience in extracting reliable data from the tests. It can be safely assumed that the trend of this curve would conform to those shown by the others. As a matter of fact, the same peculiar behavior was initially exhibited by the second curve from the top, but a later repetition of the test runs corrected this discrepancy.

The application of silicon grease to the contact joint increases the joint thermal conductance about six times, as indicated by comparison of Figs. 6 and 7. However, there is a consistent indication of a lower joint thermal conductance at 500° F as compared to that at lower temperatures. There is a possibility that partial evaporation of the grease

under the combined effects of high temperature and low pressure is causing this phenomenon. It should be pointed out that in the case of the greased specimens, the mean temperature difference across the contact joint ranged from 0.4° to 5° F, with opposing individual thermocouples occasionally indicating an unexpected increase in temperature in the direction of the heat flow. Thus, the accuracy of the absolute values is highly dubious.

In the thermal scaling of contact thermal conductance of bolted joints, some encouraging results were obtained. According to Eq 16 of Ref. 1, the ratio of thermal conductances of two joints of identical geometry is given by

$$\frac{h_m}{h_p} = \left(\frac{K_m}{K_p}\right) \left(\frac{P_m}{P_p}\right) \left(\frac{H_p}{H_m}\right) \left(\frac{a_p}{a_m}\right) \tag{6}$$

where subscripts m and p denote properties associated with the model and the prototype, respectively. For parameters on the right side of the equation, K and H are properties of material, a_i is a function of the machine finish and P is a parameter that is controllable in operation. With a_p and a_m (Figs. 19 and 20) measured from precise profilometer readings and H_p and H_m (Table 5) as properties proportional to the ultimate strength converted from measured Rockwell hardnesses, the ratio of thermal conductances of Specimens 1 and 5 under vacuum condition is

$$\frac{h_m}{h_p} = \left(\frac{P_m}{P_p}\right) \left(\frac{K_m}{K_p}\right) \left(\frac{H_p}{H_m}\right) \left(\frac{a_p}{a_m}\right) = 1 \times \frac{135}{16} \times \frac{6150 \text{ kg}/\text{cm}^2}{3868 \text{ kg}/\text{cm}^2} \times$$

$$\frac{5.33 \times 10^{-3} \text{mm}}{7.92 \times 10^{-3} \text{mm}} = 9.03$$

Experimental results indicated that the ratio is 8.2 at 610° R, 8.8 at 710° R and 8.6 at 810° R. The agreement is extremely close.

Thermal scaling on the effect of size was investigated using Specimens 4 and 5. Specimen 4 (SS-304) was made with approximately the same machine finish as Specimen 5 (SS-347), but only half scale in size. However, a larger surface waviness exists in Specimen 5 as identified by comparison of Figs. 20 and 21. Thus, the thermal conductances of these two have to be compared in a macroscopic way. Based on Eq 13 of Ref. 1, the ratio of macroscopic thermal conductance of the model and the prototype is
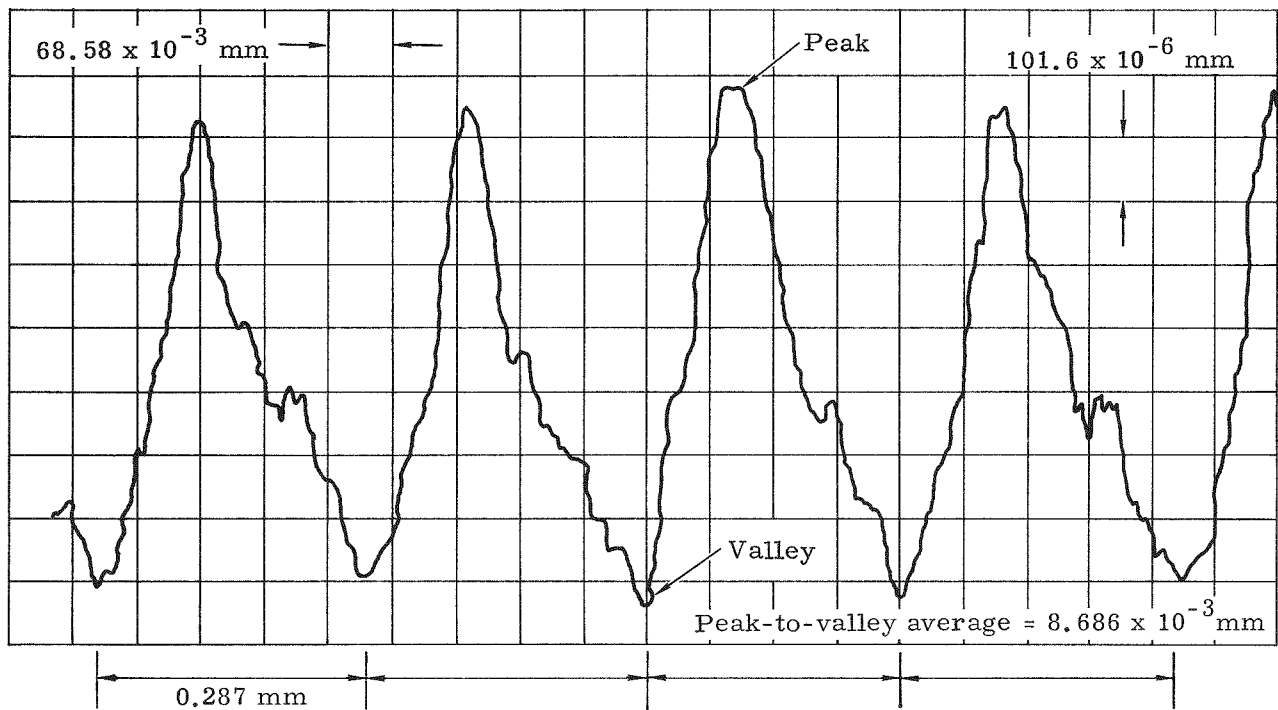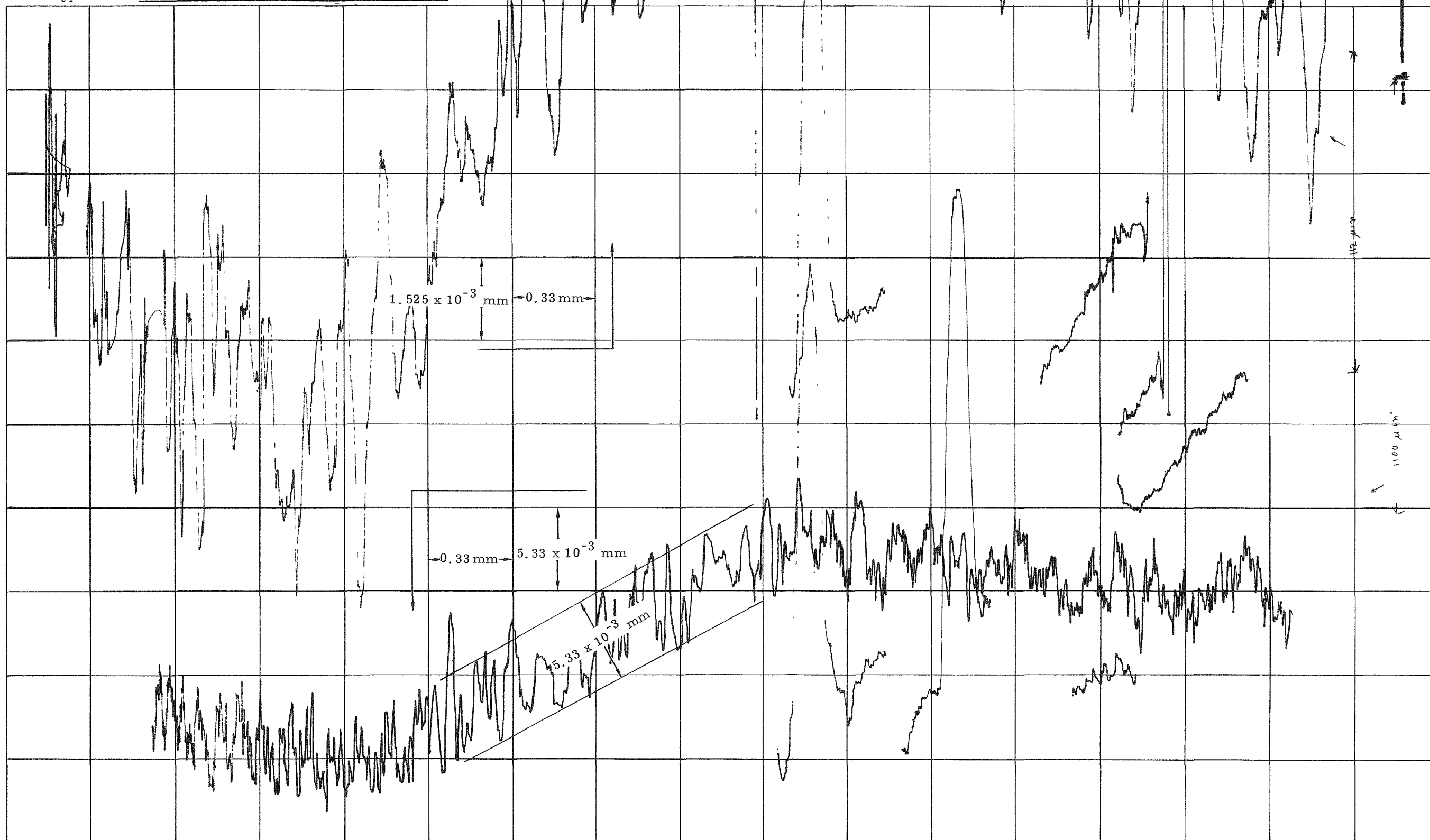
Fig. 19. Surface Profile, Specimen 1

1.525×10^{-3} mm — 0.33 mm

—0.33 mm— 5.33×10^{-3} mm

5.33×10^{-3} mm

Fig. 20. Surface Profile, Specimen 5

Date 9-9-66

Spec No. 4

Pressure

Type of test Surface Profile

1/2 scale SS 304,
high temperature side
Spec II in bag

10.1×10^{-3} mm

1/2 scale SS 304,
low temperature side
Spec I

8.53×10^{-3} mm

0.533 mm
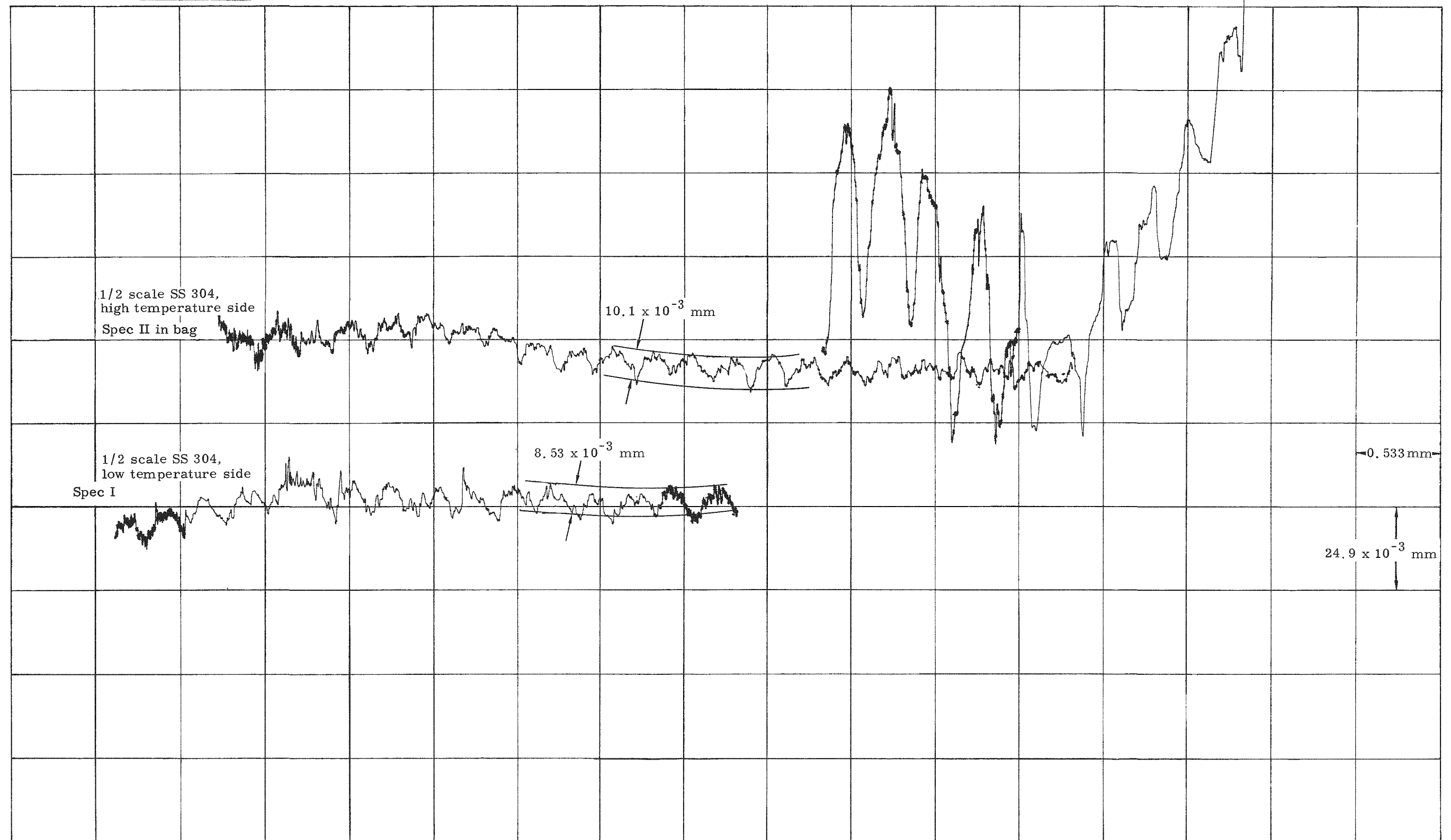
24.9×10^{-3} mm

Fig. 21.   Surface Profile, Specimen 4

$$\frac{h_m}{h_p} = \frac{K_m}{K_p} \times \frac{X_m}{X_p} \times \frac{b_p}{b_m} \times \frac{f(X_p)}{f(X_m)} \qquad (7)$$

where b denotes the radius of macroscopic contact area and X the ratio of r/b with r the radius of the area where microscopic contacts exist, as shown in Fig. 22. Function f(x) is given as

TABLE 5

Some Material Properties of Specimens

Material	Measured Rockwell Hardness	Converted Brinell Hardness No.	Converted (approximate) Ultimate Tensile Strength (kg/cm^2)
ZH62A casting	100-kg load 1/8-in. indenter E68 to 68. 5 B20	58	2110
Aluminum fitting	E96 B65	105	3868
Corrosion resistant steel fitting	B79 1/16-in. steel bar indenter	--	5270 to 7000

$$f(X) = 1 - 1.409 X + 0.0959 X 3 + \text{----------} \qquad (8)$$

Assuming the surface waviness to be of a sinusoidal nature as shown in Fig. 22, the elastic contact widths are calculated according to Hertz's theory as presented in Ref. 10. Thus,

$$\frac{h_m}{h_p} \approx \left| \times \frac{0.544 \text{ mm}/(2 \times 1.981 \text{ mm})}{0.328 \text{ mm}/(2 \times 1.981 \text{ mm})} \times \right| \times \frac{0.87}{0.79} = 1.84$$

Experimental results show a value of 2.39. This discrepancy is attributed to the instrumentation difference. Due to the small size, only four thermocouples on each plane are installed on Specimen 4 near the central portion where the temperature drop across the contact surfaces is less; on the other four specimens, six thermocouples on two concentric circles were used. If the thermal conductance of Specimen 5 was calculated from the inner thermocouples only, the ratio so obtained would be 1.72.

According to Eq 17 of Ref. 2, in cases of mechanical joints with contact surfaces coated with vacuum heat transfer grease, the thermal resistance of the joint is given as

$$R = \frac{1}{2a_s K_{ig}} + \frac{1}{2a_s K_{gj}} \tag{9}$$

where K_{ig} denotes the combined thermal conductivity of surface i and the grease and K_{gj} the thermal conductivity of the grease and surface j of the joint. Since the grease separates the two surfaces completely, the macroscopic resistance no longer exists. With K having a value of 0.126 watt/m^2-(°K/m) for the GE-683 grease, 16.1 for SS-304 and SS-347 and 135 for 2024-T4, it is evident that the thermal resistance of all greased joints will be approximately the same regardless of the joint material or pressure since the thermal resistance offered by grease is so much higher compared to that due to the metals. As shown in Fig. 7, this fact is borne out by this program. The discrepancies of Specimen 1 from those of Specimens 3 and 4 are about 23%.
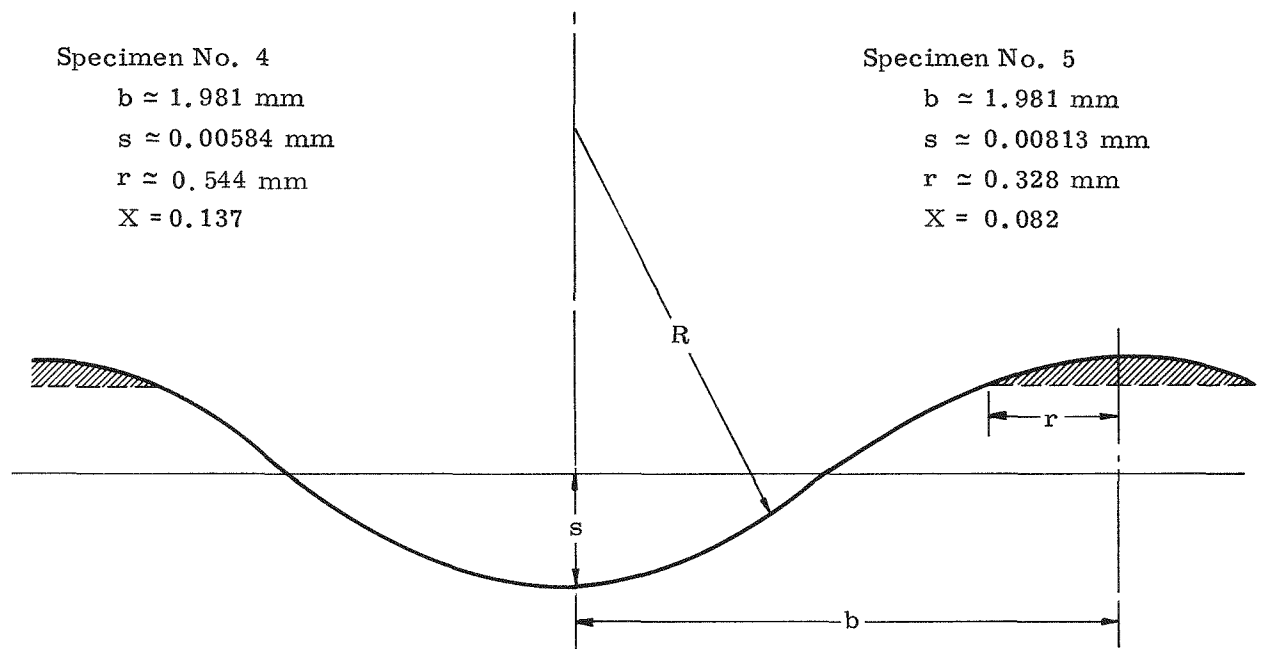
Specimen No. 4
  b ≃ 1.981 mm
  s ≃ 0.00584 mm
  r ≃ 0.544 mm
  X = 0.137

Specimen No. 5
  b ≃ 1.981 mm
  s ≃ 0.00813 mm
  r ≃ 0.328 mm
  X = 0.082

Fig. 22. Surface Geometry of Specimens 4 and 5

Fig. 23. Creep Test Specimen that Failed Before Load Application

B. MATERIAL PROPERTIES MEASUREMENTS

Material properties measurements in this program are, in general, routine with the exception of the temperature range which extended into the region close to the melting point. Some difficulties were encountered in the thermal conductivity and creep strength measurements at these elevated temperatures.

Figure 12, thermal conductivity versus temperature of ZH62A, shows the scattering of points at 500° C measured by a Martin cut bar calorimeter equipped with a guarded heater. Because of this wide scattering of data from the three specimens, some parallel experimental work was carried out in the Nuclear Research and the Thermodynamics Laboratories. All results are identified separately in Fig. 12. The dotted extension into the scattering region was drawn so it simulated the behavior of pure magnesium. It is of interest to know that the apparatus used in the Thermodynamics Laboratory was modified from the thermal conductance test apparatus to realize the desired confirmational points. However, a literature search established that the arrangement was one of the two methods recommended by the National Bureau of Standards.

On creep strength tests, it was found that at the highest temperature the specimen broke just as the load was being applied. The temperature was then reduced by an increment of 30° K for each of two additional tests, but the same phenomenon was repeated. Figure 23 shows one of the test specimen retrieved from the fixture. The fracture could have resulted from a number of causes, which included:

(1) Compression failure as a result of the difference of coefficient of expansion of the material and the threaded Inconel grip

(2) Weakening of the material at this temperature

(3) Local stress concentration due to oxidation.

Continued investigation of the cause of this failure was beyond the scope of this program and the matter was not solved.

Blank

V. CONCLUSION AND RECOMMENDATIONS

The joint thermal conductance test program was a success. Values of contact thermal conductance for three typical types of mechanical joints were obtained at four different temperatures ranging from 340° to 590° K. Joints were tested first with surfaces carefully cleaned and then again with surfaces coated with a special thermal grease similar to the type used on Nimbus B spacecraft. Except for tests with greased surfaces, scattering of experimental points from a smooth curve amounted to no more than 3%. The results of the tests conducted on the three full-scale specimens are being used for thermal analysis of Nimbus B/SNAP 19.

Thermal scaling of bolted joints was also attempted in this program for application to thermal modeling experiment (SNAP 19 Experimental Safety Program Test 4(1)(a)). Thermal scaling applied to materials of different properties deviated from Shih's scaling law (Ref. 1) for joints with identical surface geometry by less than 11% at all temperatures. Thermal scaling applied to size variation was equally successful, if proper correction is taken for the difference in instrumentation of the two specimens used. Otherwise a deviation of 30% from Shih's scaling law for joints in which macroscopic thermal restriction dominates can be encountered. For joints with contact surfaces separated by a thermal grease, it was found that the thermal conductance of all joints tested increased sixfold or more over clean surfaces and that the contact conductance is insensitive to the type of fastening, the materials forming the joint or the size of the joint. The results seem to agree well with Shih's hypothesis on greased joints in Ref. 1.

Materials properties measured at room temperatures were in general agreement with literature values. The validity of values at higher temperatures can only be judged by the trend of the property versus temperature curve and the scattering of the test points. There are two events worth mentioning. On thermal conductivity of ZH62A at temperature above 673° K, supplementary tests had to be carried out at two other laboratories to establish the trend of the curve. However, the accuracy of those points above 673° K is questionable. Values should be used with caution. On creep strength at high temperature (775° to 783° K), the specimens broke before applying the load. The cause of the failure was not identified.

A. RECOMMENDATIONS

It is highly recommended that some followup work be conducted to ascertain additional useful data which would be beneficial to both the

SNAP 19 program and future programs involving magnesium alloys and mechanical joints.

More material creep tests should be conducted at higher temperature ranges to determine the cause of failure of three specimens tested between 755° to 787° K. A new type of grip should be used to avoid compression stress developed due to differences in thermal expansion of the materials of the specimens and fixture or the thread on the grip may be relieved to eliminate such interference. Better environmental control of the test chamber should be provided to avoid reaction stress concentration.

Two different sizes of specimens should be used to check the effect of the environment on size. A total of 12 tests should be conducted.

Additional test runs should be conducted on mechnical joint Specimens 1, 4 and 5 with and without heat transfer grease between the contact surfaces. A few of the early runs in this program should be repeated to check the validity. More runs should be made to check the effect of contact pressure on thermal conductance. The pressure effect was not investigated in this program because it was originally aimed specifically for application to the particular design.

Two three-bolt specimens should be fabricated and tested to investigate the restraining effect of neighboring bolts on the thermal conductance of a bolted joint.

VI. REFERENCES

1. Shih, C., "Thermal Similitude of Manned Spacecraft." AIAA Paper 66-22.

2. Gabron, F., Johnson, R. W., Vickers, J. M. F., and Lucas, J. W., "Thermal Scale Modeling of the Mariner IV Spacecraft." AIAA Paper 66-22.

3. Clausing, A. M. and Chao, B. T., "Thermal Contact Resistance in a Vacuum Environment." ME-TN-242-1 Engineering Experiment Station, University of Illinois.

4. Hultberg, J. A., "Thermal Joint Conductance." Personal correspondence.

5. Timoshenko, S., Strength of Materials, Part II; Advanced Theory and Problems. D. Van Nostrand Company, Inc., 1941.

6. Aron, W. and Colombo, G., "Controlling Factors of Thermal Conductance Across Bolted Joints in a Vacuum Environment." ASME Paper 63-WA-196.

7. Elliott, D. H., "Thermal Conduction Across Aluminum Bolted Joints." ASME Paper 65-HT-53.

8. Fenech, H., Henry, J. J., and Rohsenow, W. M., Thermal Contact Resistance. Chapter 13, "Development in Heat Transfer." MIT Press, 1964.

9. Shlykov, Yu. P. and Ganin, Ye. A., "Thermal Resistance of Metallic Contacts." Journal of Heat Mass Transfer, Vol 7, pp 921 to 929.

10. Roark, R. J., Formulae for Stress and Strain. McGraw-Hill Book Company, 3rd edition.